Supplementary Information

Autofluorescent antimalarials by hybridization of artemisinin and coumarin:

In vitro/*in vivo* studies and live-cell imaging

Lars Herrmann,[a] Maria Leidenberger,[b] Adrielle Sacramento de Morais,[c] Christina Mai,[a] Aysun Çapci,[a] Mariana da Cruz Borges Silva,[c] Fabian Plass,[d,e] Axel Kahnt,[d,e] Diogo R. M. Moreira,[*c] Barbara Kappes [*b] and Svetlana B. Tsogoeva [*a]

[a.] *Organic Chemistry Chair I and Interdisciplinary Center for Molecular Materials (ICMM), Friedrich-Alexander-Universität Erlangen-Nürnberg, Nikolaus-Fiebiger-Straße 10, 91054 Erlangen, Germany, svetlana.tsogoeva@fau.de*
[b.] *Institute of Medical Biotechnology, Friedrich-Alexander-Universität Erlangen-Nürnberg, Paul-Gordon-Straße 3, 91052 Erlangen, Germany, barbara.kappes@fau.de*
[c.] *Instituto Gonçalo Moniz, Fundação Oswaldo Cruz, Salvador 40296-710, Brazil, diogo.magalhaes@fiocruz.br*
[d.] *Leibniz Institute of Surface Engineering (IOM), Permoserstrasse 15, 04318 Leipzig, Germany*
[e.] *Physical Chemistry Chair I, Friedrich-Alexander-Universität Erlangen-Nürnberg, Egerlandstrasse 3, 91058 Erlangen, Germany*

Table of content

1. General information

All reactions were performed in distilled and dried or HPLC grade solvents under N_2. The reagents supplied from commercial sources were used without further purification. TLC chromatography was performed on precoated aluminium silica gel SIL G/UV254 plates (Macherey-Nagel & Co.) and the detection occurred *via* fluorescence quenching or development in a molybdato phosphate solution (10% in EtOH). All compounds were dried in high-vacuum (10^{-3} mbar). ^{1}H NMR and ^{13}C NMR spectra were recorded at room temperature on a Bruker Avance or JEOL JNM GX 400 spectrometer operating at 300, 400 or 600 MHz, 75, 100 or 125 MHz. All chemical shifts are given in the ppm-scale and refer to the nondeuterized proportion of the solvent. ESI, APPI and MALDI mass spectra were recorded on a Bruker Daltonik maXis 4G or Bruker Daltonik micrOTOF II focus. Elemental analysis (C, H, N) were carried out with an Euro EA 3000 (EuroVector) machine and an Elementar vario MICRO cube machine and calculated values confirm a purity of > 95% for the all biologically tested compounds. Artesunic acid and dihydroartemisinin were purchased from ABCR (Karlsruhe, Germany) and TCI (Deutschland GmbH). The coumarin azide **11** was purchased from Biosynth Carbosynth. The synthesis of starting materials **7**[1, 2], **9**[1] and **10**[3] was described earlier in literature.

2. Synthesis and characterization of the hybrids

Synthesis of Hybrid **1**:

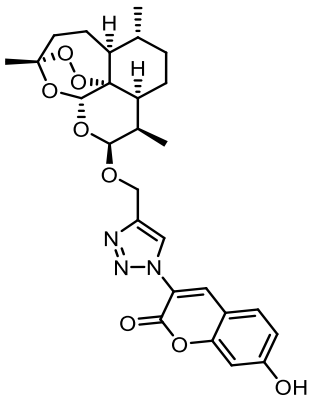

$CuSO4•5H_2O$ (7.65 mg, 30.0 µmol, 10 mol%) and sodium ascorbate (12.3 mg, 60.0 µmol, 20 mol%) were dissolved in 3 mL H_2O (bubbled with N_2 for 30 min.). After the catalyst mixture turned brown and subsequently orange a mixture of the DHA-derived alkyne **7** (100 mg, 310 µmol, 1.0 equiv.) and coumarin-azide **11** (63.0 mg, 310 µmol, 1.0 equiv.) in 3 mL DCM (bubbled with N_2 for 30 min.) were added and the reaction mixture was stirred at r.t. overnight. Afterwards the mixture was extracted with DCM (3x 25 mL), the combined organic phases were washed with H_2O (25 mL) and Brine (25 mL) and dried over $MgSO_4$. After removal of the solvent under reduced pressure, the residue was purified by column chromatography (3:2//hexane/EtOAc) to give the product **1** in 45% (72.2 mg, 138 µmol) as an off-white solid. ^{1}H NMR (400 MHz, DMSO) δ 10.89 (s, 1H), 8.58 (d, J = 25.8 Hz, 2H), 7.75 (d, J = 8.6 Hz, 1H), 6.91 (dd, J = 8.5, 2.3 Hz, 1H), 6.85 (d, J = 2.3 Hz, 1H), 5.48 (s, 1H), 4.92-4.81 (m, 2H), 4.60 (d, J = 12.3 Hz, 1H), 2.48-2.39 (m, 1H), 2.20 (td, J = 14.0, 3.9 Hz, 1H), 2.06-1.96 (m, 1H), 1.87-1.76 (m, 1H), 1.71 (td, J = 13.4, 3.4 Hz, 1H), 1.65-1.57 (m, 1H), 1.56-1.48 (m, 1H), 1.47-1.27 (m, 6H), 1.19-1.09 (m, 1H), 0.89 (d, J = 6.4 Hz, 3H), 0.82 (d, J = 7.4 Hz, 3H). ^{13}C NMR (101 MHz, DMSO) δ 162.4, 156.3, 154.6, 144.2, 136.3, 130.9, 124.7, 119.4, 114.3, 110.4, 103.4, 102.2, 100.2, 87.1, 80.5, 60.1, 52.1, 43.8, 36.6, 36.0, 34.1, 30.4, 25.6, 24.3, 24.0, 20.1, 12.7. HRMS (ESI+) m/z calculated for $C_{27}H_{31}N_3NaO_8$ $[M+Na]^+$: 548.2002, found: 548.2003. Elemental analysis; calculated for $C_{27}H_{31}N_3O_8$: C: 61.71 H: 5.95 N: 8.00 found: C: 61.61 H: 6.07 N: 7.80.

Synthesis of Hybrid **2**:

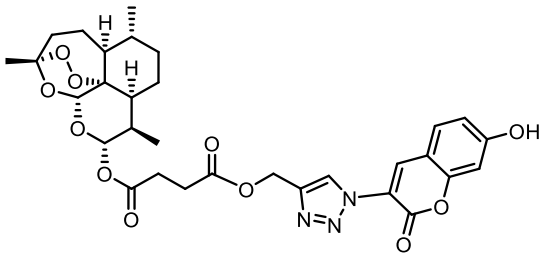

DMF (3 mL) was bubbled through with argon for 10 min. under stirring. Subsequently $CuSO_4$ (x5 H_2O, 8.86 mg, 35.5 µmol, 0.2 equiv.) was added to form a light blue solution. The reaction was stirred for 5 min. before ascorbic acid (12.5 mg, 71.0 µmol, 0.4 equiv.) was added. Afterwards the alkyne **9** (90.0 mg, 213 µmol, 1.2 equiv.) and the coumarin-azide **11** (36.1 mg, 178 µmol, 1 equiv.) were added, and the reaction mixture was stirred for 1 h at r.t. After the completion of the reaction was proven via TLC, it was diluted with DCM (25 mL) and washed the water (20 mL). The aqueous phase was extracted with DCM (2x 25 mL), the combined organic phase was dried over $MgSO_4$ and concentrated under reduced pressure. The crude product was purified via column chromatography (hexane:EtOAc//1:1) to obtain the final product **2** as a white solid (42.3 mg, 67.6 µmol, 38%). ^{1}H NMR (400 MHz, DMSO-d6): δ 10.93 (s, 1H), 8.61 (d, J = 6.9 Hz, 2H), 8.27 (s, 1H), 7.75 (d, J = 8.6 Hz, 1H), 6.91 (dd, J = 8.5, 2.3 Hz, 1H), 6.85 (d, J = 2.2 Hz, 1H), 6.79 (d, J = 4.8 Hz, 1H), 5.25 (s, 3H), 2.73-2.60 (m, 4H), 2.44-2.36 (m, 1H), 2.36-2.23 (m, 1H), 2.17-2.05 (m, 2H), 2.04 (s, 3H), 2.01-1.92 (m, 1H), 1.81-1.72 (m, 1H), 1.65-1.21 (m, 5H), 0.98 (d, J = 5.8 Hz, 3H), 0.93 (d, J = 6.9 Hz, 3H); ^{13}C NMR (101 MHz, $CDCl_3$): δ 212.3, 210.3, 171.9, 170.9, 161.6, 159.8, 156.4, 154.9, 142.8, 134.7, 130.6, 125.0, 119.8, 115.0, 111.3, 103.4, 91.8, 57.9, 57.1, 52.1, 41.4, 40.8, 36.6, 34.7, 31.2, 30.1, 29.1, 28.8, 20.6, 20.2, 11.6; HRMS (APPI) calculated for $C_{31}H_{36}N_3O_{11}$ $[M+H]^+$: 626.2344; found: 626.2358. Elemental analysis; calculated: C: 59.5 H: 5.64 N: 6.72; found: C: 59.4 H: 5.81 N: 6.60.

Synthesis of Hybrid **8**:

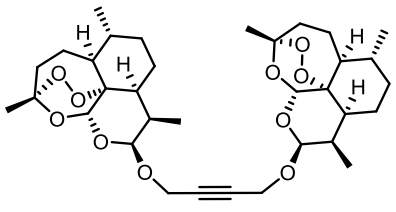

DHA (1.25 g, 4.40 mmol, 2.0 equiv.) and but-2-yne-1,4-diol (190 mg, 2.20 mmol, 1.0 equiv.) were suspended in dry Et_2O (100 mL) under N_2. The suspension was stirred for 10 min. at r.t. before BF_3 xEt_2O (434 µL, 500 mg, 3.52 mmol, 1.6 equiv.) was added. With addition of BF_3 xEt_2O a clear solution in formed. The solution was stirred for 24 h before it was quenched with $NaHCO_3$ solution (50%, 100 mL). The aqueous phase was extracted with Et_2O (3x 150 mL), and the combined organic phase was dried over $MgSO_4$ and concentrated under reduced pressure.

The crude product was purified via column chromatography (hexane:EtOAc//4:1) to obtain the product (*β,β*-diastereomer) as a white solid (610 mg, 986 µmol, 45%). ^{1}H NMR (400 MHz, $CDCl_3$): *δ* 5.39 (s, 2H), 4.96 (d, J = 3.7 Hz, 2H), 4.40-4.25 (m, 4H), 2.72-2.59 (m, 2H), 2.36 (ddd, *J* = 14.6, 13.4, 4.0 Hz, 2H), 2.03 (ddd, *J* = 14.6, 4.9, 2.9 Hz, 2H), 1.93-1.83 (m, 2H), 1.78-1.71 (m, 4H), 1.64 (dq, *J* = 13.2, 3.4 Hz, 2H), 1.55-1.41 (m, 10H), 1.39-1.28 (m, 2H), 1.28-1.17 (m, 2H), 0.98-0.81 (m, 14H); ^{13}C NMR (101 MHz, $CDCl_3$): *δ* 104.3, 100.6, 88.2, 82.0, 81.2, 55.3, 52.7, 44.5, 37.5, 36.6, 34.7, 30.8, 26.3, 24.8, 24.6, 20.5, 13.0; HRMS (APPI) calculated. for $C_{33}H_{37}N_2NaO_8$ $[M+Na]^+$:641.3296; found: 641.3297. Elemental analysis; calculated: C, 66.00; H, 8.15; N, 0.00; found: C: 66.2 H: 8.19; N, 0.00.

Synthesis of Hybrid **3**:

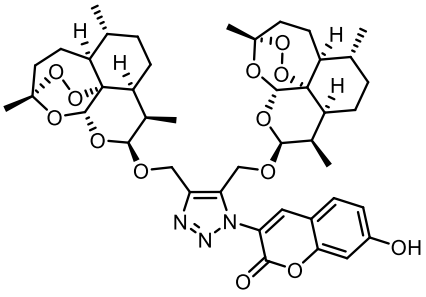

Cp*RuCl(COD) (2.46 mg, 6.46 µmol, 0.02 equiv.) was dissolved in dry DMF (10 mL, bubbled through with argon under stirring for 15 min.). To the light brown solution, the alkyne **8** (200 mg, 323 µmol, 1.0 equiv.) and the coumarin-azide **11** (65.7 mg, 323 µmol, 1.0 equiv.) were added. The reaction turns into a dark red solution and is stirred under argon at r.t. for 24 h. The reaction mixture was diluted with DCM:MeOH (5:1, 30 mL) and washed with H_2O (15 mL). The aqueous phase was extracted with DCM (2x 25 mL) and the combined organic phase was dried over $MgSO_4$ and concentrated under reduced pressure. The crude product was purified via column chromatography (hexane:EtOAc//1:1) to obtain the product **3** as a white solid (106 mg, 129 µmol, 40%). ^{1}H NMR (400 MHz, DMSO-d6): *δ* 11.03 (s, 1H), 8.54 (s, 1H), 7.69 (d, *J* = 8.6 Hz, 1H), 6.92 (dd, *J* = 8.5, 2.3 Hz, 1H), 6.85 (d, *J* = 2.2 Hz, 1H), 5.44 (s, 1H), 5.05 (s, 1H), 4.97-4.82 (m, 3H), 4.72 (d, *J* = 3.6 Hz, 1H), 4.62 (dd, *J* = 12.6, 4.3 Hz, 2H), 2.48-2.40 (m, 1H), 2.36-2.27 (m, 1H), 2.26-2.07 (m, 2H), 2.06-1.98 (m, 1H), 1.97-1.89 (m, 1H), 1.86-1.77 (m, 1H), 1.75-1.59 (m, 3H), 1.56-1.49 (m, 1H), 1.48-0.96 (m, 17H), 0.94-0.83 (m, 4H), 0.80 (d, *J* = 7.4 Hz, 3H), 0.74 (d, *J* = 6.1 Hz, 4H), 0.71-0.62 (m, 1H), 0.58 (d, *J* = 7.3 Hz, 3H); ^{13}C NMR (101 MHz, $CDCl_3$): *δ* 162.7, 157.1, 155.9, 143.1, 140.7, 134.9, 130.5, 120.2, 115.1, 110.9, 104.4, 103.6, 102.6, 102.0, 88.2, 88.0, 81.3, 80.9, 60.5, 59.1, 52.7, 52.4, 44.5, 44.1, 37.4, 36.6, 36.4, 34.7, 34.4, 31.0, 30.7, 26.3, 26.1, 24.8, 24.6, 24.4, 22.5, 20.5, 20.4, 14.2, 13.13, 12.8; HRMS (APPI) calculated for $C_{43}H_{55}N_3NaO_{13}$ $[M+Na]^+$: 844.3627; found: 844.3641. Elemental analysis; calculated: C: 62.8 H: 6.75 N: 5.11 found: C: 62.4 H: 6.79 N: 5.11.

Synthesis of Hybrid **4:**

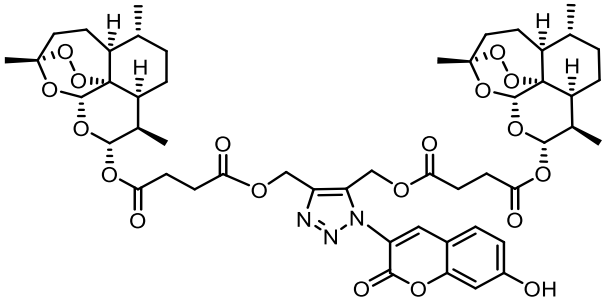

Compound **4**: In a dried flask the catalyst Cp*Ru(cod)Cl (1.00 mg, 2.90 µmol, 2 mol%) was dissolved in 15 mL anhydrous DMF (bubbled with argon for 15 min.) and the artemisinin derived alkyne **10** (330 mg mg, 403 µmol, 1.0 equiv.) and coumarin azide **11** (81.9 mg, 403 µmol, 1.0 equiv.) were added. The mixture was stirred overnight at r.t.. The solvent was removed under reduced pressure and the crude product was purified by column chromatography (hexane/EtOAc 2:3). The hybrid **4** was obtained in 61% (252 mg, 247 µmol) as off-white solid. ^{1}H NMR (400 MHz, DMSO) δ 11.04 (s, 1H), 8.49 (s, 1H), 7.71 (d, *J* = 8.6 Hz, 1H), 6.93 (dd, *J* = 8.5, 2.3 Hz, 1H), 6.87 (d, *J* = 2.2 Hz, 1H), 5.66 (d, *J* = 9.7 Hz, 1H), 5.58 (d, *J* = 9.7 Hz, 1H), 5.55 (s, 1H), 5.50 (s, 1H), 5.32-5.20 (m, 4H), 2.74-2.61 (m, 4H), 2.58-2.51 (m, 4H),2.36-2.11 (m, 4H), 2.03-1.93 (m, 2H), 1.86-1.75 (m, 2H), 1.69-1.10 (m, 20H), 1.01-0.81 (m, 8H), 0.76 (d, *J* = 7.1 Hz, 3H), 0.68 (d, *J* = 7.1 Hz, 3H). ^{13}C NMR (101 MHz, DMSO) *δ* 171.7, 171.2, 170.8, 170.6, 163.3, 157.1, 155.7, 142.9, 140.9, 133.4, 131.4, 117.7, 114.4, 110.1, 103.6, 102.4, 91.9, 91.8, 90.6, 90.6, 79.8, 79.8, 56.5, 53.5, 51.1, 44.6, 44.5, 36.0, 35.9, 33.7, 33.5, 31.6, 31.5, 28.6, 28.4, 28.3, 28.1, 25.5, 24.2, 21.7, 21.0, 20.0, 13.9, 11.7, 11.6. HRMS (ESI+) m/z calculated for $C_{51}H_{63}N_3NaO_{19}$ $[M+NA]^+$: 1044.3936, found: 1044.3948. Elemental analysis; calculated for $C_{51}H_{63}N_3O_{19}$: C: 59.93 H: 6.21 N: 4.11 found: C: 60.28 H: 6.58 N: 4.01.

Synthesis of Hybrid **5**:

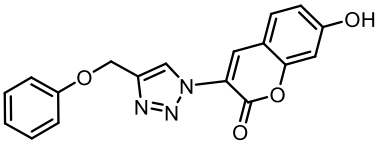

DMF (3 mL) was bubbled through with argon for 10 min. under stirring. Subsequently $CuSO_4$ (x5 H_2O, 25.2 mg, 101 µmol, 0.2 equiv.) was added to form a light blue solution. The reaction was stirred for 5 min. before ascorbic acid (35.5 mg, 202 µmol, 0.4 equiv.) was added. Afterwards prop-2-yn-1-yl benzoate (100 mg, 757 µmol, 1.5 equiv.) and the coumarin-azide **11** (102 mg, 504 µmol, 1 equiv.) were added, and the reaction mixture was stirred for 1 h at r.t. After the completion of the reaction was proven via TLC, it was diluted with DCM (25 mL) and washed the water (10 mL). The aqueous phase was extracted with DCM:MeOH (10:1; 2x 25 mL), the combined organic phase was dried over $MgSO_4$ and concentrated under reduced pressure. The crude product was purified via column chromatography (hexane:EtOAc//2:3) to obtain the final product **5** as an off-white solid (62.3 mg, 186 µmol, 37%). ^{1}H NMR (400 MHz, DMSO-d6): *δ* 10.92 (s, 1H), 8.68 (s, 1H), 8.62 (s, 1H), 7.75 (d, *J* = 8.6 Hz, 1H), 7.37-7.27 (m, 2H), 7.10-7.05 (m, 2H), 7.01-6.94 (m, 1H), 6.91 (dd, *J* = 8.5, 2.3 Hz, 1H), 6.85 (d, *J* = 2.3 Hz, 1H), 5.25 (s, 2H); ^{13}C NMR (101 MHz, DMSO-d6): *δ* 200.2, 195.6, 194.0, 192.3, 180.6, 174.2, 168.6, 167.2, 163.2, 158.6, 156.9, 152.3, 152.0, 148.0, 139.8, 98.3; HRMS (APPI) calculated for $C_{18}H_{14}N_3O_4$ $[M+H]^+$: 336.0979; found: 336.0988. Elemental analysis; calculated: C, 64.5; H, 3.91; N, 12.5; found: C, 64.4; H, 3.95; N, 12.3.

Synthesis of Hybrid **6**:

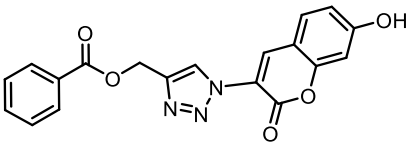

DMF (3 mL) was bubbled through with argon for 10 min. under stirring. Subsequently $CuSO_4$ (x5 H_2O, 10.4 mg, 41.6 µmol, 0.2 equiv.) was added to form a light blue solution. The reaction was stirred for 5 min. before ascorbic acid (14.7 mg, 83.2 µmol, 0.4 equiv.) was added. Afterwards prop-2-yn-1-yl benzoate (50.0 mg, 312 µmol, 1.5 equiv.) and the coumarin-azide **11** (42.3 mg, 208 µmol, 1 equiv.) were added, and the reaction mixture was stirred for 1 h at r.t. After the completion of the reaction was proven via TLC, it was diluted with DCM (25 mL) and washed the water (10 mL). The aqueous phase was extracted with DCM (2x 25 mL), the combined organic phase was dried over $MgSO_4$ and concentrated under reduced pressure. The crude product was purified via column chromatography (hexane:EtOAc//1:2) to obtain the final product **6** as a white solid (21.7 mg, 59.7 µmol, 29%). ^{1}H NMR (400 MHz, DMSO-d6): *δ* 10.94 (s, 1H), 8.70 (s, 1H), 8.63 (s, 1H), 8.02-7.95 (m, 2H), 7.75 (d, *J* = 8.6 Hz, 1H), 7.70-7.65 (m, 1H), 7.58-7.50 (m, 2H), 6.91 (dd, *J* = 8.6, 2.3 Hz, 1H), 6.85 (d, *J* = 2.3 Hz, 1H), 5.51 (s, 2H); ^{13}C NMR (101 MHz, DMSO-d6): *δ* 165.5, 162.6, 156.3, 154.7, 142.1, 136.5, 133.6, 131.0, 129.3, 129.3, 128.8, 125.9, 119.2, 114.3, 110.3, 102.2, 57.7; HRMS (ESI) calculated for $C_{19}H_{13}N_3NaO_5$ $[M+Na]^+$: 386.074741; found: 386.073688. Elemental analysis; calculated: C, 62.81; H, 3.61; N, 11.57; found: C, 62.77; H, 3.76; N, 11.21.

3. Biological methods

Assessment of antiplasmodial activity *in vitro*

***In vitro* antimalarial activity assay**

P. falciparum 3D7, Dd2, and K1 parasites were cultured in type A-positive human erythrocytes at a hematocrit of 5% in RPMI 1640 supplemented with 25 mM HEPES, 2 mM l-glutamine, 24 mM $NaHCO_3$, 0.1 mM hypoxanthine, 25 µg/mL gentamycin and 0.5% albumax I. Cultures were incubated at 37 °C under controlled atmospheric conditions of 3% O_2, 5% CO_2, and 92% N_2 at 95% relative humidity. Cultures used in cell proliferation assays were synchronized by sorbitol treatment. [4] Concentrations to inhibit parasite growth by 50% (EC_{50}) were determined using the SYBR Green I malaria drug sensitivity assay.[5]100 µl aliquots of a cell suspension containing ring stages at a parasitemia of 0.2% and a hematocrit of 2% were added to the wells of 96-well microtiter plates. Plates were incubated for 72 h in the presence of different drug concentrations. Subsequently, cells of each well were lysed with 100 µl lysis buffer (40 mM Tris, pH 7.5, 10 mM EDTA, 0.02% saponin, 0.08% Triton X-100) containing 8.3 µM SYBR green. Plates were incubated for 1 h in the dark at room temperature under constant mixing before fluorescence (excitation wavelength 485 nm; emission wavelength 520 nm) was determined using a microtiter plate fluorescence reader (Victor X4; Perkin Elmer). Drugs were serially diluted 1:3 with initial drug concentrations being 243 nM for artesunic acid and its derivates, 81 nM for dihydroartemisinin and 243 nM for its derivates and 243 nM for chloroquine when the strain 3D7 was used and 729 nM when Dd2 and K1 strains were examined. Each drug concentration was examined in triplicate and repeated at least three times. Uninfected erythrocytes (hematocrit 2%) and infected erythrocytes without drug served as controls and were investigated in parallel. Percent growth was calculated as described by Beez.[6] Data were analyzed using the SigmaPlot (version 12.0; Hill function, three parameters) and Sigma Stat programs.

Speed of antiplasmodium action

The compounds were suspended in DMSO and then diluted in serial two-fold dilutions in RPMI-1640 medium using 96-well flat-bottom microplates until achieving seven desired concentrations. Additionally, 100 µL of a 3D7 strain asynchronous culture of *P. falciparum* with 1-1.5% parasitemia and 1% final hematocrit were added into the plates containing 100 µl of each hybrid compound concentration in duplicate, and then incubated for 24 or 72 h at 37 °C and with gas mixture. DHA was used as positive control (fast-acting drug) and ATO was used as negative control (relatively slow-acting drug). Untreated parasite received 100 µL of medium. Parasite growth was determined by Nucleic Acid Gel Stain (Invitrogen) method using a microplate reader Sinergy 4 (Biotek), and the antimalarial activity was expressed as 50% inhibitory concentrations (IC_{50}), where each IC_{50} value was represented as the mean and standard deviation of at least two independent experiments performed.

Drug degradation in RBC culture

The relative drug concentration of hybrids in the erythrocyte culture was estimated by measuring the antiplasmodium activity of supernatant harvested from erythrocyte culture as described previously.[7] In brief, a 96-well flat-bottom microplate, 125 µL of hybrid compounds or DHA were aliquoted in sextuplicate, and then 125 µL of uRBC (2% hematocrit) were added into the microplate. DHA was employed as a short-living drug while amodiaquine (AQ) was employed as a standard drug (long-lasting drug). Final concentration of all drugs was of at 500 nM. The plate was incubated at 37 °C and in the standard gas mixture for different times (0.16, 6 and 24 h). Drug exposure times of 0.16, 6 and 24 h for uRBC were carefully chosen by having in mind that the elimination half-life time ($t_{1/2}$) of DHA in the plasma is closer to 1-3 h. Untreated uRBCs incubated at the same timeframe were used as negative controls. After each timepoint, supernatants were collected and stored until use.

Supernatants were diluted in medium for a serial two-fold dilutions and at least six different supernatant dilutions were aliquoted in the plate. The antiplasmodium activity of supernatant was determined by incubation of with 1-2% parasitemia and 2.5%

hematocrit for 72 h at the same condition described above using 3D7 strain. After incubation, the plate was frozen at -80 °C overnight, and then thawed at 37 °C for 4 h. In addition, 100 µL of each respective well were transferred to a black sterile 96-well plate, and 100 µL of a SYBR Green I solution (0.2 µL of SYBR Green I per 1 mL of lysis buffer) were aliquoted. The plate was incubated at room temperature protected from light, and gently mixed using a shaker for 1 h. The fluorescence measurement was performed using excitation and emission wavelengths of 485 and 530 nm, respectively. Only the experiments where the IC_{50} of supernatant harvested at 10 min displayed values similar to the IC_{50} of a fresh drug dilution in the medium were considered for analysis of equivalent drug concentration. Therefore, by considering that the supernatant harvested at 10 min has a 500 nM of drug concentration, an equivalent drug concentration was calculated as $500/IC_{50}$ value for each indicated time. At least three independent experiments were performed.

Cytotoxicity against mammalian cells (CC_{50})

In vitro cytotoxicity was assayed against the lineage of J774 murine cells. Cell culture was maintained in DMEM (J774) containing 10% fetal bovine serum and supplemented with L-glutamine, vitamins and amino acids in 75-cm^2 flasks at 37 °C, with the medium changed twice weekly. Cell cultures from 60 to 80% confluence were trypsinized, washed in complete medium, and 4x 10^4 cells were plated in 100 µL per well with complete medium in 96-well flat-bottom white plates for 24 h at 37 °C prior to the addition of the compounds. Triplicate aliquots of compound and the reference drugs (stock solution in DMSO) covering six different concentrations at 2-fold dilutions were added to the wells, and plates were incubated for 72 h at 37 °C. Following incubation for 72 h at 37 °C, the plates were maintained at room temperature, the culture medium was removed, and 100 µL from the CellTiter-Glo kit was added to each well. Bioluminescence was measured using a Filtermax™ F5 Multi-Mode microplate reader (Molecular Devices, San Jose, USA) and Softmax software. CC_{50} data were obtained from using Prism version 5.01. The selectivity index (S.I.) was estimated using the CC_{50}s from mammalian cells divided by the IC_{50} obtained against the asexual blood stage *P. falciparum*.

Drug uptake measured by microplate fluorometer

Blood was harvested from *P. berghei*-infected mice and a solution containing 1% final hematocrit and 5% parasitemia was aliquoted to each well. A 0.2 mL cells volume in 96-well plates was incubated with different concentrations of compounds, ranging from 12 to 0.75 µM, at indicated times (0.16 h to 2 h). Afterwards, plate was centrifuged, supernatant (extracellular phase) was removed and transferred into another new plate. Cell pellet was firstly washed with complete medium and with saline for two times, then the remaining cell pellet (intracellular phase) was suspended with water, frozen and heated twice for cell lyse. Fluorescence was measured using a Fluoroskan DCA-0595 microplate reader (PerkinElmer) at excitation and emission wavelengths of 355 nm and 460 nm, respectively. Each drug concentration was tested in triplicate. Each experiment was performed independently three times. To adjust any difference in absorption and emission properties among the compounds, we initially subtracted the drug fluorescence reading from a blank control (DMSO only) and then the values were normalized. Only the experiments where the relative fluorescence units (RFU) of the sum (supernatant and cell pellet fraction) displayed values similar to a standard drug-concentration curve of a freshly prepared drug dilution in the medium without cells were considered for analysis of drug uptake. Uptake was then calculated using the equation $\{=(Q_2*100)/(Q_2+Q_1)\}$, where Q_1 is the supernatant (extracellular phase) and Q_2 is the cell pellet (intracellular phase).

Drug uptake measured by flow cytometry

It was determined following prior protocols[8]. Blood was harvested from *P. berghei*-infected mice and a solution containing 1% final hematocrit and 5% parasitemia was aliquoted to each well. A 1 mL cells volume in 24-well plates was incubated with different concentrations of compounds, ranging from 12 to 0.75 µM, at indicated times (0.5 h to 2 h). Afterwards, samples were washed with sterile saline, incubated with SYTO-61 at 5.0 µM (for iRBC) for 30 min. in the dark. Samples were washed and placed in polypropylene tubes and the cells were resuspended in 1 mL isoton diluent. 10.000 events were respectively acquired using a BD LSRFortessa™ Cell Analyzer (BD, New Jersey, USA). Parasites were identified by the GFP signal in the FITC

channel (gain of 500 V) and parasites were identified by SYTO-61 staining quantified in the APC channel (gain of 450 V). The intrinsic fluorescence of compounds was detected in the pacific blue channel (gain of 527 V) and adjusted in comparison to cells without treatment (untreated). No spillover into these channels was observed. For the competition experiments, DHA was added at the indicated concentration 30 min. prior to adding compounds, and data acquisition was performed as described above. Each drug concentration was tested in triplicate and each experiment was performed independently three times. Uptake was calculated using the equation {=(Q_2*100)/(Q_2+Q_1)}, where Q_2 is the cells positively stained for compound and Q_1 is the cells negatively stained for compound.

In vivo blood schizontocidal activity

Male Swiss mice (4-6 weeks) were infected by intraperitoneal injection of 10^6 NK65/GFP strain *P. berghei*-infected erythrocytes and randomly divided into groups of *n*=5. Each drug was solubilized in DMSO/saline (20:80 v/v) prior administration. Treatment was initiated within 2 h (orally by gavage) or 24 h (by subcutaneous injection) post-infection and given daily for four consecutive days of a 100 µL volume. Artesunate (ARE) treated mice were used as positive control group, while untreated infected mice were used as negative control group. The following parameters were evaluated: parasitemia counted at 4, 5, 6, 7 and 8 days post-infection and 30 days post-infection animal survival. The % of parasitemia reduction was calculated as follows ([mean vehicle group − mean treated group)/mean vehicle group] × 100%). Each experiment was performed using no more than four groups. An end-point to interrupt the experiment was defined as mice with symptoms of severe anemia, which were euthanized prior the end of experiment. Experiments were conducted in 2019-2022 in accordance with the recommendations of Ethical Issues Guidelines and were approved (protocol 020/2018) by the local Animal Ethics Committee at Fiocruz Bahia (IGM, Salvador, Brazil).

In vivo cell imaging: Cultivation of parasites

Plasmodium falciparum strain 3D7 was cultivated in RPMI 1640 medium containing 2 mM L-glutamine, 25 mM 4-(2-hydroxyethyl)-1-piperazineethanesulfonic acid (HEPES) and 24 mM $NaHCO_3$ supplemented with 0.1 mM hypoxanthine, 25 µg/mL gentamicin and 0.5% AlbuMAX® I containing 5% (v/v) in A+ erythrocytes. Cultures were grown in an atmosphere of 5% O_2, 3% CO_2 at 37 °C. Under these conditions, the duration of the intraerythrocytic growth cycle of the 3D7 strain is 44 h. For the drug experiments, asynchronous cultures with 5% parasitaemia were used.

In vivo cell imaging: Fluorescence microscopy

An asynchronous culture was incubated with 200 nM **1** at 37 °C for 30 min, 2 h, 4 h or 8 h. Tissue culture chambers were coated with 0.01% poly D-Lysine in ultrapure H_2O for 30 min and washed three times with PBS. Costaining was performed with 300 nM Syto 13 (nucleic acid stain; Thermofisher) and 30 nM Nile Red (lipid stain, Sigma). 4 µl of infected red blood cells, treated with **1** for the above given time periods, were diluted with 1 ml ringer solution supplemented with 300 nM Syto13 and 30 nM Nile Red, transferred into a 1 ml culture chamber and incubated 5-10 min at 37 °C. For life cell imaging, an Eclipse Ti microscope (Nikon, Düsseldorf) was used with 1000x magnification. To detect respect fluorescences, the following settings for excitation and emission were used: **1** - Ex 387 nm/Em 440 nm, Syto 13 - Ex 485 nm/Em 529 nm and Nile Red - Ex 560 nm/Em 607 nm.

Table S1: Speed of the *in vitro* antiparasitic activity, cytotoxicity for J774 mammalian cells and selectivity indexes of compounds.

Compounds	IC_{50} for 3D7 strain of *P. falciparum* (mean±S.D. in nM) [a]		CC_{50} for J774 cells (mean 95 % CI, in μM)[b]	Selectivity index (S.I.)[c]
	24 h	72 h		
1	1.0 ±0.5	0.8 ±0.3	9.56 (9.01-10.14)	11950
2	101 ±22	62.7 ±10	37.6 (26.3-53.1)	600
3	0.58 ±0.2	0.7 ±0.4	5.21 (4.55-5.97)	7442
4	8.9 ±2.1	5.3 ±1.8	32.8 (28.2-38.0)	6037
5	N.D.	5250 ±410	> 80	N.D.
6	N.D.	> 10000	> 80	N.D.
ATO	6.5 ±0.3	0.4 ±0.09	N.D.	N.D.
DHA	25.2 ±3.9	5.8 ±1.0	51.3 (37.6-67.4)	8844
GV	-	-	4.91 (3.70-5.12)	N.D.

[a]Assay performed against asexual blood stages (asynchronous culture). Drugs were incubated at indicated times (24 or 72 h) and then parasitemia was determined using SYBR green I. Values are the fifty percent inhibitory concentration (IC_{50}) and expressed as mean ± standard deviation (S.D.) of two independent experiments (each concentration in duplicate). Relatively slow-acting drug ATO and fast-acting drug DHA were tested in parallel. [b]Values are the fifty percent cytotoxic concentration (CC_{50}) and expressed as mean (95 % CI) values of one single experiment, each concentration in triplicate. J774, murine macrophage cells. [c]Selectivity index was calculated as CC_{50} (J774)/IC_{50} 72 h (*P. falciparum*). DHA = Dihydroartemisinin; ATO = Atovaquone. GV = gentian violet. N.D. = not determined.

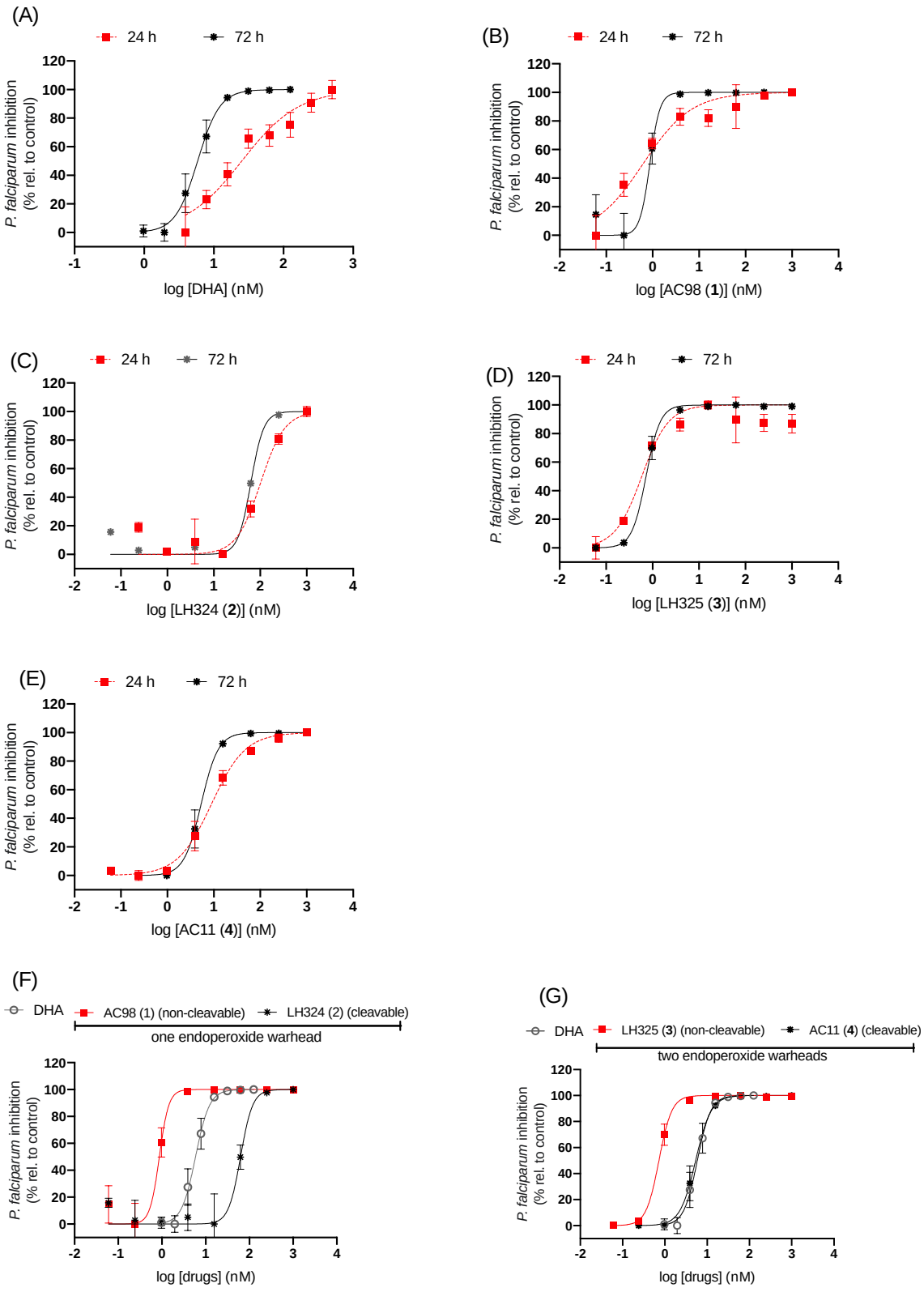

Fig S1: Panels A to E: Representative curve concentration-response for DHA or the hybrid compounds against the asynchronous culture of 3D7 strain of *P. falciparum*. Parasites were incubated for 24 or 72 h. Data were fitted to the log(concentration) versus response with a variable slope equation in GraphPad Prism and replicate data was collected to calculate IC_{50} values. Panel F: comparison of the activity for hybrid compounds containing only one singe endoperoxide warhead. Panel G: comparison of the activity for hybrid compounds containing two endoperoxide warheads.

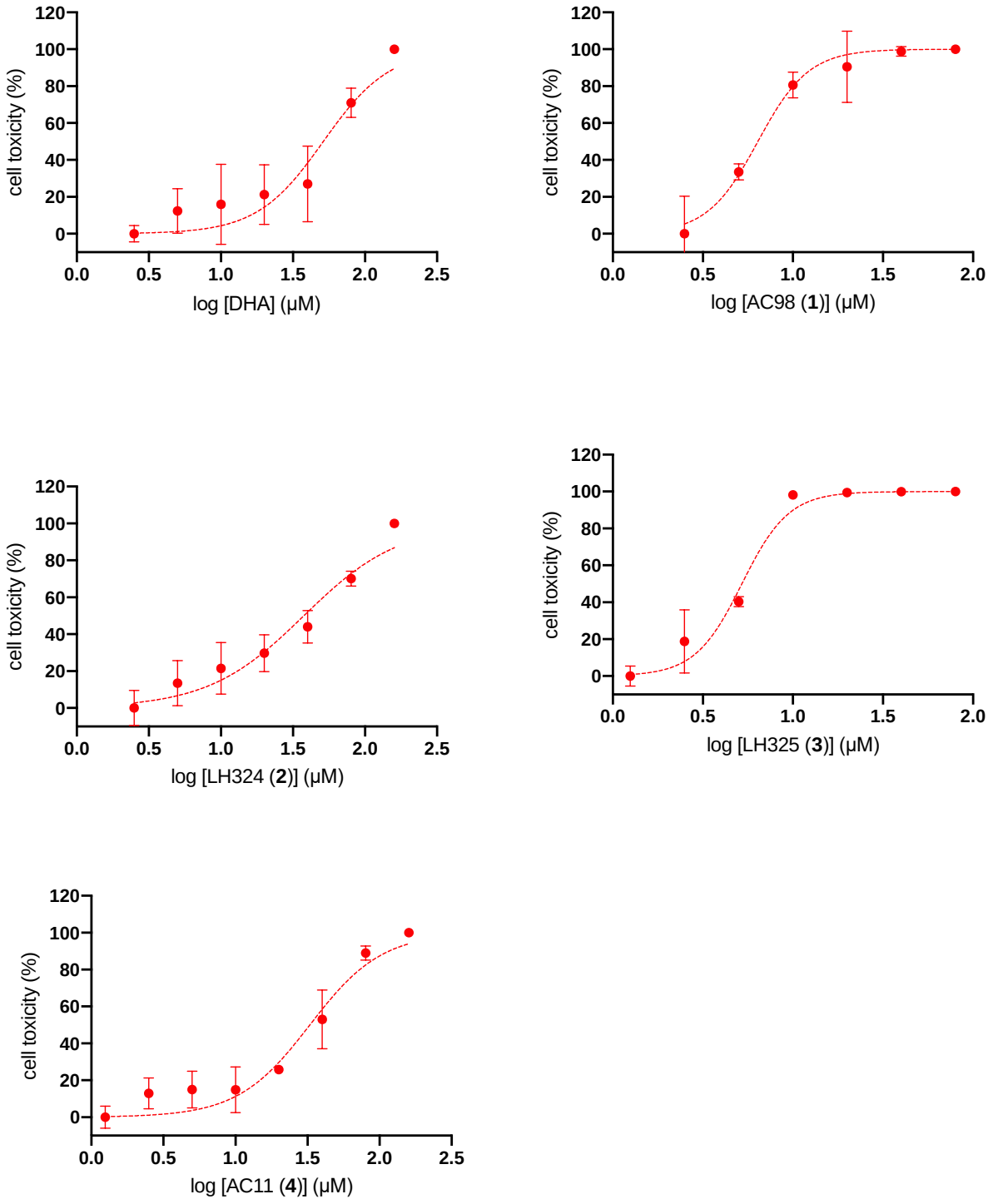

Fig S2 Representative curve concentration-response for DHA or the hybrid compounds **1**-**4** for the determination of cell toxicity for J774 cell lineage. Cells were incubated for 72 h. Data were fitted to the log(concentration) versus response with a variable slope equation in GraphPad Prism and replicate data was collected to calculate CC_{50} values.

Table S2 *In vivo* efficacy of endoperoxide drugs in *P. berghei*-infected mice.

Compounds	Dose in mg/kg (μmol/kg)[a]	Inhibition (% vs CTRL) [b]	Median of animal survival in days (cure, %)[c]
treatment orally by gavage			
Vehicle (untreated)	-,-	-,-	20 (0 %)
Artesunate (ARE)	25 (65)	88.5 ±2.9	28 (0 %)
1	35 (65)	81.9 ±2.2	32 (0 %)
4	66 (65)	86.5 ±1.0	32 (0 %)
treatment subcutaneous			
Artesunate (ARE)	8.5 (22)	>99	30# (50%)
1	11.5 (22)	>99	> 30# (100%)
2	14 (22)	41.7 ±8.0	18 (0 %)
3	18 (22)	>99	> 30# (100%)
4	22 (22)	94 ±11	26 (25 %)
	66 (65)	96 ±2.0	> 30# (100%)

[a]Treatment was given after 2 h (orally by gavage) or 24 h (subcutaneous injection) post-infection once-a-day for four consecutive days. [b]Parasitemia inhibition was determined in comparison to vehicle (untreated), determined 48 h after the last day of drug administration and values are mean ± standard deviation. [c]Animal survival was monitored up to 30 days. Values are from one single experiment, using n = 5/group. # p = 0.05 (Log-rank and Mantel-Cox test) *versus* vehicle.

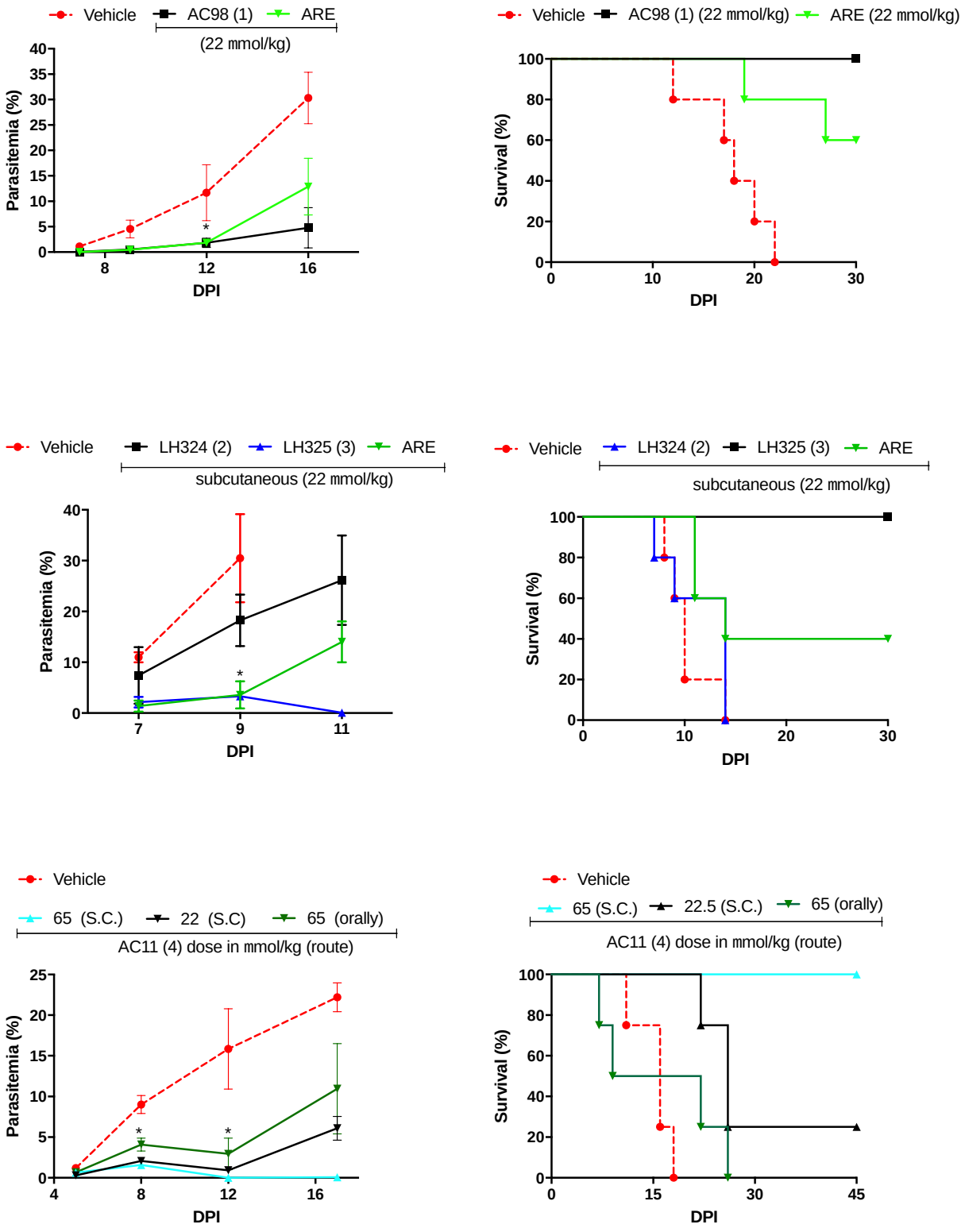

Fig S3 Representative curves of parasitemia and animal survival from the *in vivo* efficacy study of endoperoxide drugs in *P. berghei*-infected mice. Unless indicated, drug dosage was given by subcutaneous route of administration at the dose of 22 μmol/kg of animal weight. ARE = Artesunate.

Table S3 The table summarizes the IC_{50} values and the fold change of the antimalarial activity.

Compounds	Antiplasmodium activity (IC_{50}, nM) of the supernatant from uRBC[a]			Fold change (24 h /0.16 h)[b]
	0.16 h	6 h	24 h	
1 (AC98)	1.2±0.1	1.5±0.02	3.5±1.7	2.9
2 (LH324)	66±11	196±30.7*	349± 79**	5.2
3 (LH325)	1.1±0.4	1.3±0.3	2.8±0.5	3.1
4 (AC11)	3.8±0.7	5.9±2.1	30.1±9.2**	7.9
Amodiaquine (AQ)[c]	3.6 (3.3-4.3)	3.8 (3.5-4.0)	3.3 (2.2-3.4)	0.9
DHA	6.7±2.5	22.7±3.1*	147.3±10.3**	21.9

Values are the median ± standard error of the mean (S.E.M.) of three independent experiments (each concentration in duplicate).
[a]The *in vitro* antiparasitic activity of supernatants against the 3D7 strain of *P. falciparum* determined 72 h after drug exposure to the parasites.
[b]Calculated as the ratio between IC_{50} values of 24 h versus 0.16 h.
[c]Values are expressed as mean (95 % CI) of one single experiment, each concentration in duplicate. Unpaired two-tailed *t*-test at 95% confidence interval: **p* < 0.05; ***p* < 0.001 versus IC_{50} (0.16 h).

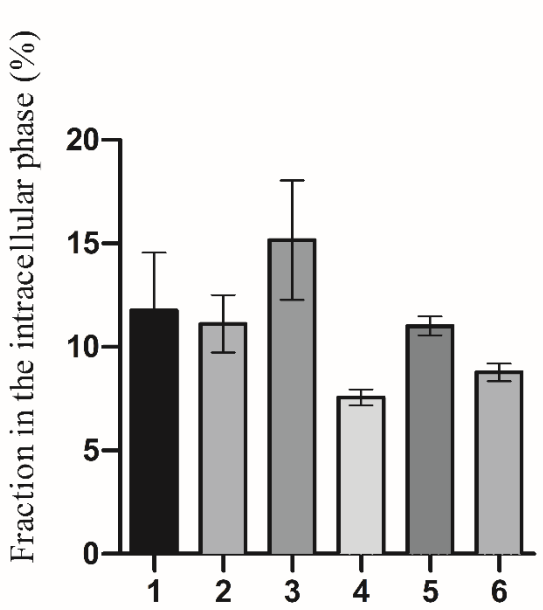

Fig. S4 Fraction (%) of the drugs in the intracellular phase. Assay was determined in *P. berghei*-infected cells and measured in a microplate fluorometer. Asynchronous culture of *P. berghei*-infected cells (5% of parasitemia, 2.5% hematocrit) were incubated in the presence of drugs (3.0 μM) for 1 h. Values are expressed as mean (95% CI) of one single experiment, each concentration in triplicate.

(A)

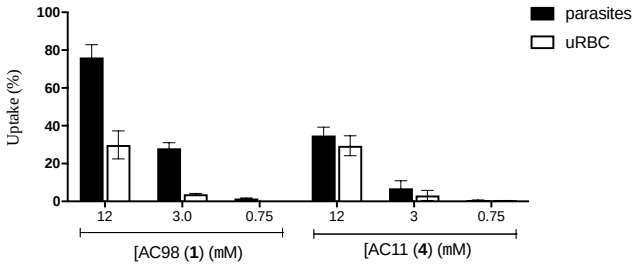

(B)

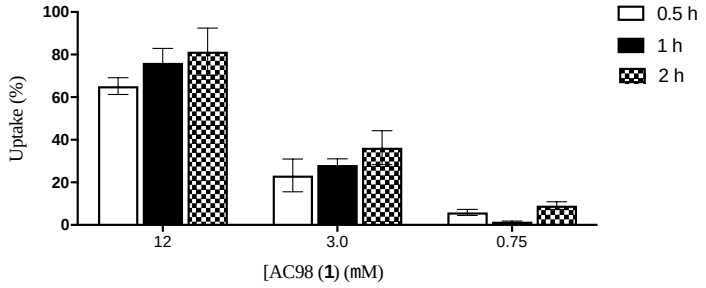

(C)

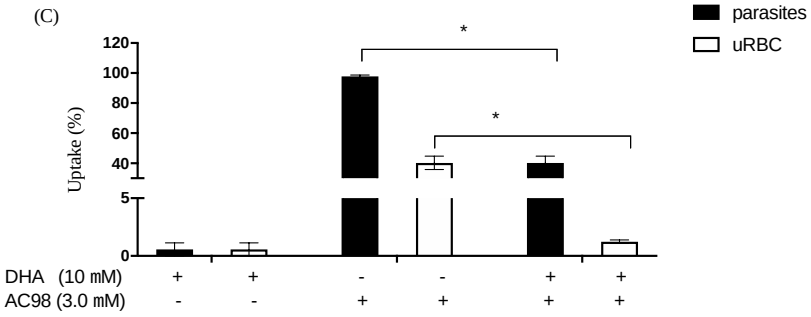

(D)

Parameters (%)	Treatment (3 μM) [a]	
	AC98 (1)	AC11 (4)
Uptake in the uRBC	3.8±0.3	3.1±2.0
Uptake in the parasites	28.2±2.0	7.0±3.0
Blockage of uptake for uRBC under DHA pre-exposure [b]	71.5	N.D.
Blockage of uptake for parasites under DHA pre-exposure	58.8	N.D.

Fig. S5 The profile of drug uptake in *P. berghei*-infected cells. Panel A shows that the uptake is concentration dependent. Panel B depicts a time-dependency uptake in the parasites. Panel C show that the uptake decreases upon DHA pre-exposure. Asynchronous culture of *P. berghei*-infected cells (5 % of parasitemia, 2.5 % hematocrit) were incubated in the presence of drugs for 1 h unless indicated. Parasites (GFP^+) and uRBC (GFP^-) were gated and the % of cells stained for the fluorescent drugs (AC98 or AC11) were assessed by flow cytometry. In panels A and B, the % uptake is relative to the entire population (unstained parasites, stained parasites, unstained uRBC, stained uRBC). In panel C, drug uptake was determined by the % of stained versus unstained cells. Panel D: a table summarizing the parameters. Footnotes: [a,b] Values were determined in the presence of drugs for 1 h of incubation period. Values are the mean and standard deviation of two independent experiments, each experiment with two technical replicates. * $p < 0.05$ (unpaired two-tailed *t*-test at 95 % confidence interval). Parasites = *P. berghei*-infected RBC. uRBC = uninfected red blood cells.

Associated discussion to Fig. S5

Although hybrid **1** had its cellular localization in *P. falciparum* precisely profiled at clinically relevant nanomolar concentrations, a remaining question was that the lipophilicity by which these hybrid compounds can enter in the cells and become bioavailable to the parasite might be dissimilar than DHA. To exclude that lipophilicity is shifting the cellular localization and distribution of **1** in comparison to DHA, we further profiled the drug uptake by incubating the parasites to the drugs and estimated the fraction of parasites scored as fluorescence-positive parasites per unit time (also referred to as the % of uptake). To screen the uptake for all hybrids, it was detected by a fluorescence microplate reader. Results have shown that the percentage of drug uptake for the intracellular phase did not significantly differ among the hybrid compounds (Supplementary Fig. 5). To discern the drug uptake in host cells (uRBC) from infected cells (parasites), a flow cytometry analysis was employed. By estimating the proportion of stained to unstained parasites, it was established that the drug uptake rate for the parasites was gradual, since a concentration-dependent response is observed for both **1** and **4** (Supplementary Fig. 5). By estimating the proportion of stained parasites at different times, it was concluded that uptake occurs in a few seconds and that over time the percentage of stained parasites gradually increases, and this is steady at approximately 1 h; so, this time frame was employed for the subsequent competition experiments. The competition experiment has revealed that pre-incubation with DHA did decrease the uptake of **1** in both uRBC and parasites. The results of uptake, using drug concentration in micromolar range that mimics the treatment in patients, are suggestive that any dissimilarity in lipophilicity among the hybrids is not significant to substantially change the drug uptake among compounds and to subsequently explain the drug potency. More importantly, the existing competition between DHA and **1** revealed that the mechanism of cellular uptake and diffusion in the host cells and then in the parasites is in common for these two drugs.

4. Fluorescence measurements:

Photophysics:

All compounds were measured in methanol. Absorption spectra were recorded using a UV-2101PC (Shimadzu) UV-vis spectrometer. Fully corrected fluorescence spectra were measured using a Fluoromax 4 (Horiba). The fluorescence quantum yield was determined by the comparative method by Williams et. al.[9] using 9,10 diphenylanthracene in cyclohexane with a fluorescence quantum yield of 0.90 as reference compound.[10]

Fluorescence time profiles were measured with a Fluoromax 4 (Horiba) in the TCSPC mode exciting the samples with a 370 or 405 nm NanoLED (Horiba). The fluorescence lifetimes were obtained by deconvolution of the fluorescence time profiles with the instruments response function (IRF) and fitting to a monoexponential function.

Hybrid 1:

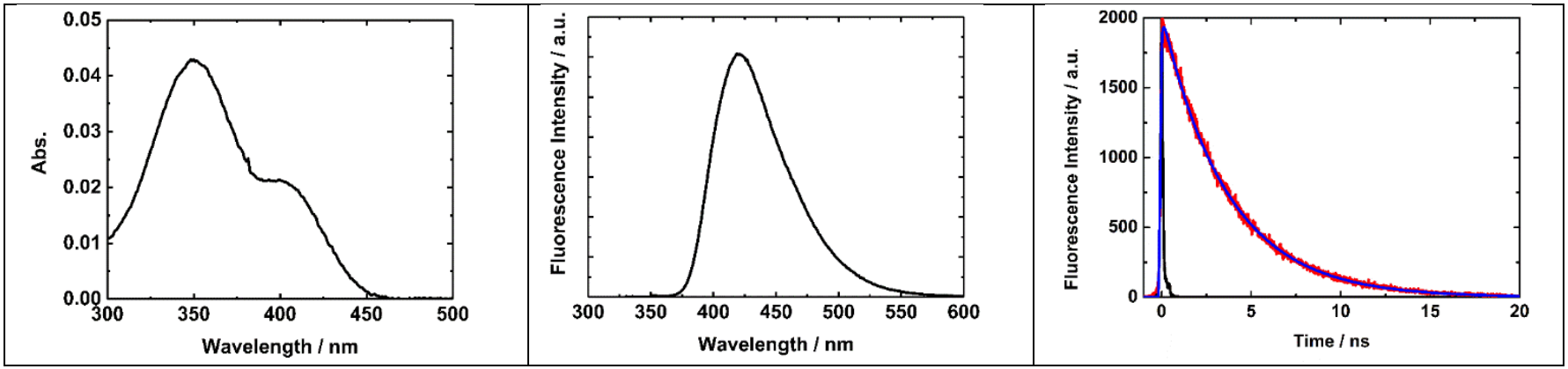

Fig. S6 left: Absorption spectrum of **1** in methanol. **Middle:** Fluorescence spectrum of **1** in methanol upon photoexcitation at 320 nm. **Right:** Fluorescence time profiles of **1** measured in methanol (red) at 435 nm upon photoexcitation at 405 nm. The black curve depicts the instruments response function (IRF) and the blue curve represents the result of the deconvolution with the IRF and the monoexponential fit of the measured time profile.

Hybrid 2:

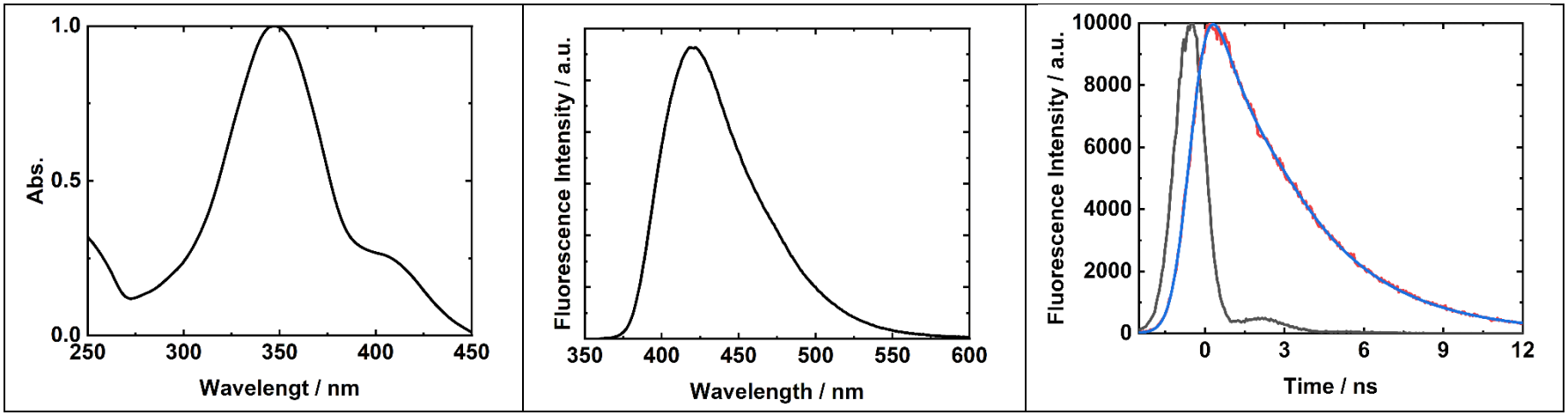

Fig. S7 left: Absorption spectrum of **2** in methanol. **Middle:** Fluorescence spectrum of **2** in methanol upon photoexcitation at 350 nm. **Right:** Fluorescence time profiles of **2** measured in methanol (red) at 410 nm upon photoexcitation at 370 nm. The black curve depicts the instruments response function (IRF) and the blue curve represents the result of the deconvolution with the IRF and the monoexponential fit of the measured time profile.

Hybrid 3:

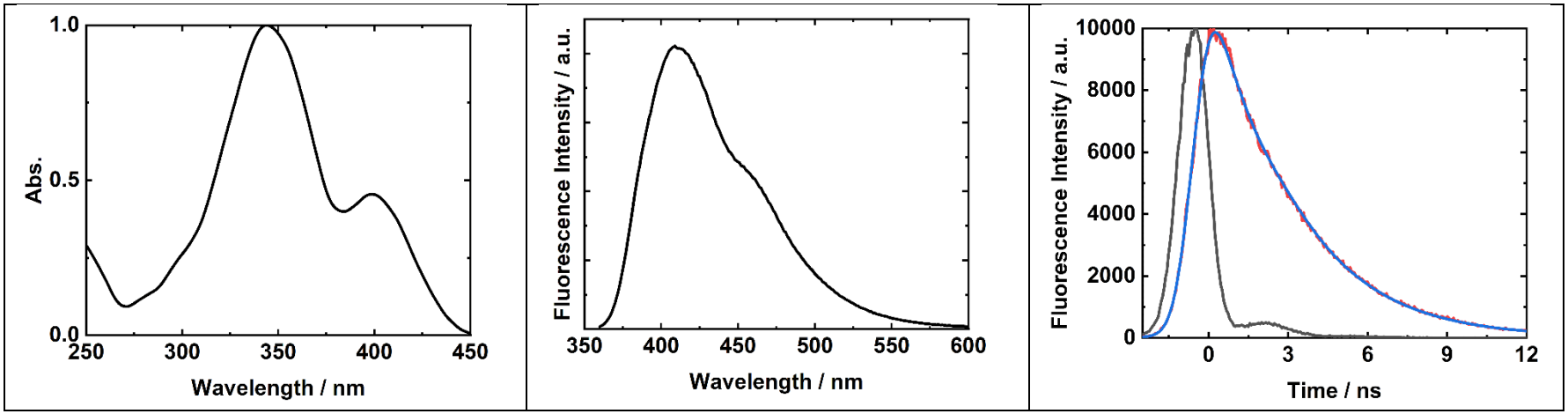

Fig. S8 left: Absorption spectrum of **3** in methanol. **Middle:** Fluorescence spectrum of **3** in methanol upon photoexcitation at 350 nm. **Right:** Fluorescence time profiles of **3** measured in methanol (red) at 410 nm upon photoexcitation at 370 nm. The black curve depicts the instruments response function (IRF) and the blue curve represents the result of the deconvolution with the IRF and the monoexponential fit of the measured time profile.

Hybrid 4:

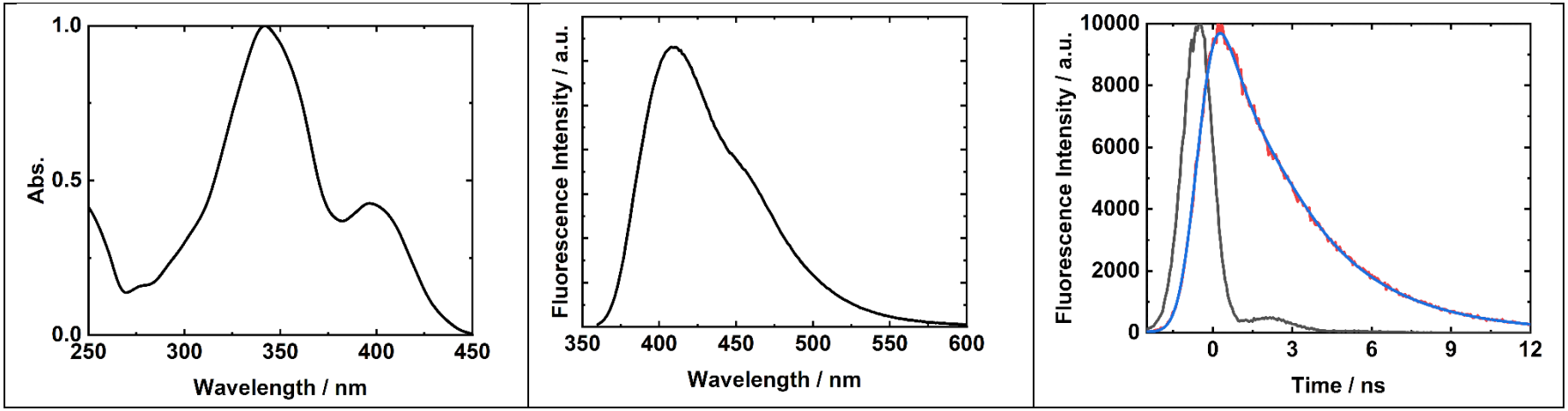

Fig. S9 left: Absorption spectrum of **4** in methanol. **Middle:** Fluorescence spectrum of **4** in methanol upon photoexcitation at 350 nm. **Right:** Fluorescence time profiles of **4** measured in methanol (red) at 410 nm upon photoexcitation at 370 nm. The black curve depicts the instruments response function (IRF) and the blue curve represents the result of the deconvolution with the IRF and the monoexponential fit of the measured time profile.

Compound 5:

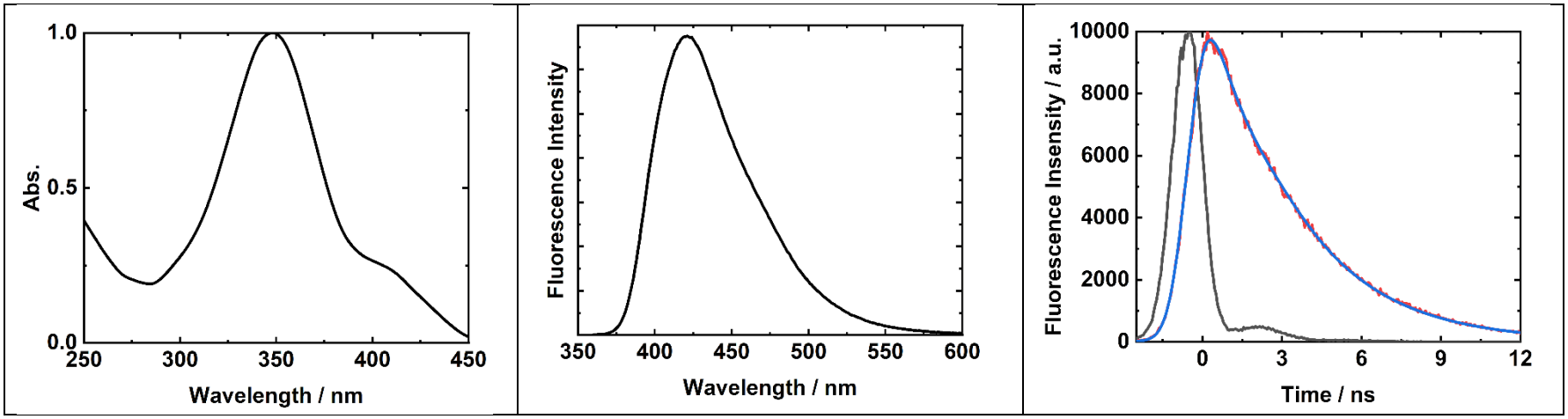

Fig. S10 Left: Absorption spectrum of **5** in methanol. **Middle:** Fluorescence spectrum of **5** in methanol upon photoexcitation at 350 nm. **Right:** Fluorescence time profiles of **5** measured in methanol (red) at 410 nm upon photoexcitation at 370 nm. The black curve depicts the instruments response function (IRF) and the blue curve represents the result of the deconvolution with the IRF and the monoexponential fit of the measured time profile.

Compound 6:

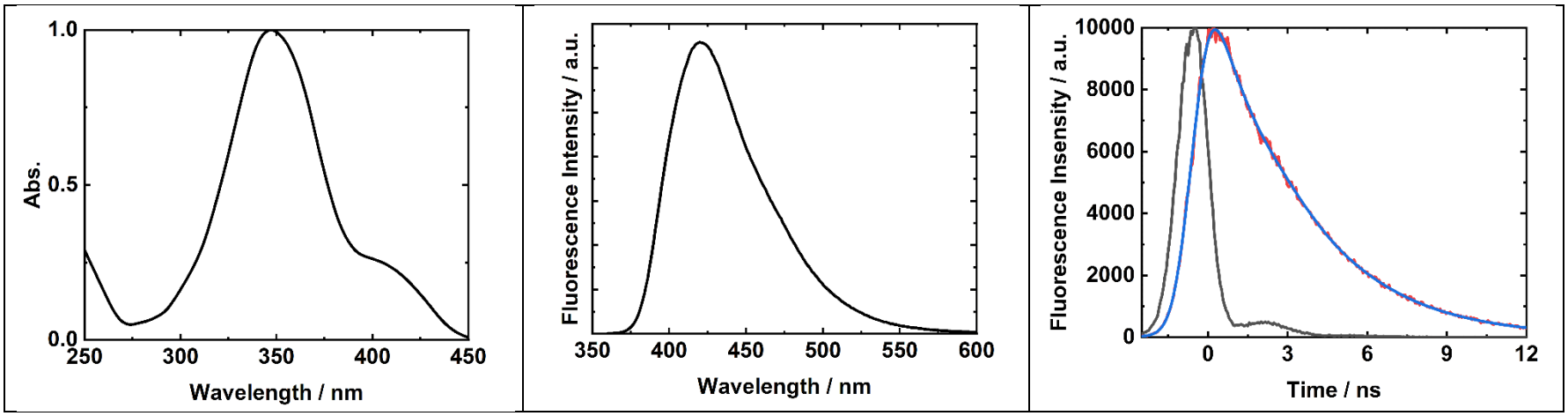

Fig. S11 Left: Absorption spectrum of **6** in methanol. **Middle:** Fluorescence spectrum of **6** in methanol upon photoexcitation at 350 nm. **Right:** Fluorescence time profiles of **6** measured in methanol (red) at 410 nm upon photoexcitation at 370 nm. The black curve depicts the instruments response function (IRF) and the blue curve represents the result of the deconvolution with the IRF and the monoexponential fit of the measured time profile.

5. ^{1}H and ^{13}C NMR spectra:

^{1}H NMR (400.35 MHz, DMSO-d6) of 1:

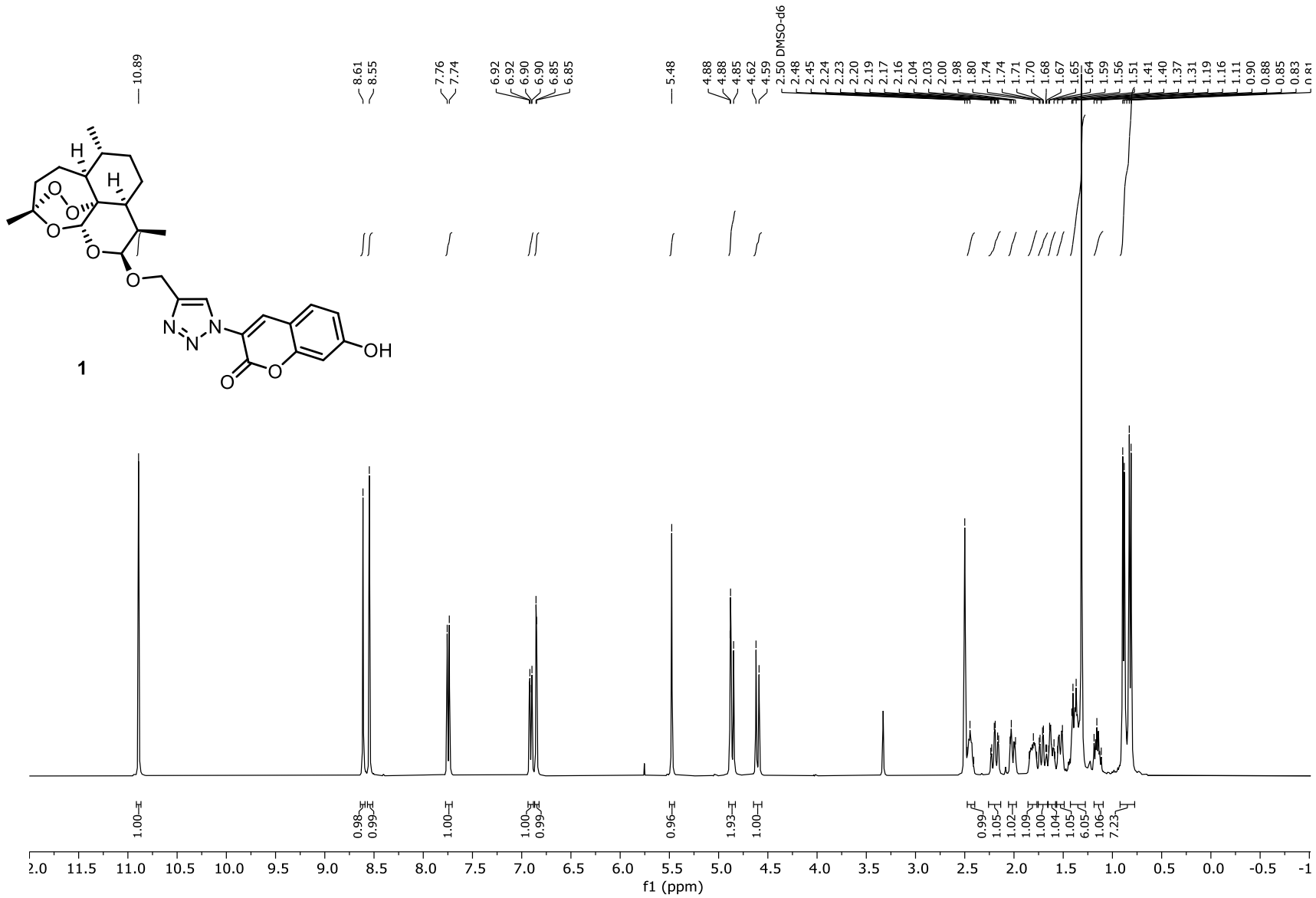

^{13}C NMR (100.68 MHz, DMSO-d6) of 1:

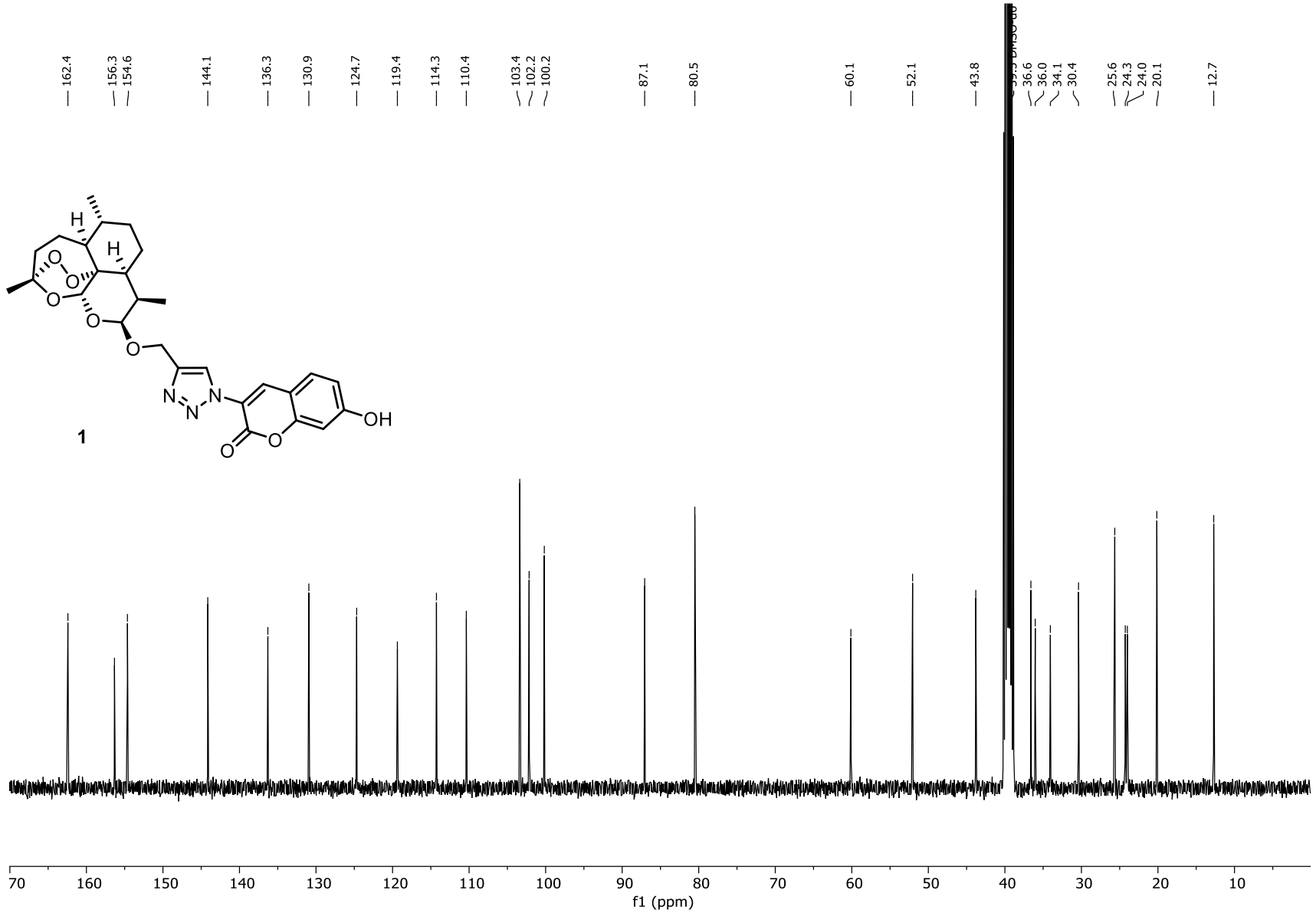

^{1}H NMR (400.35 MHz, $CDCl_3$) of 9:

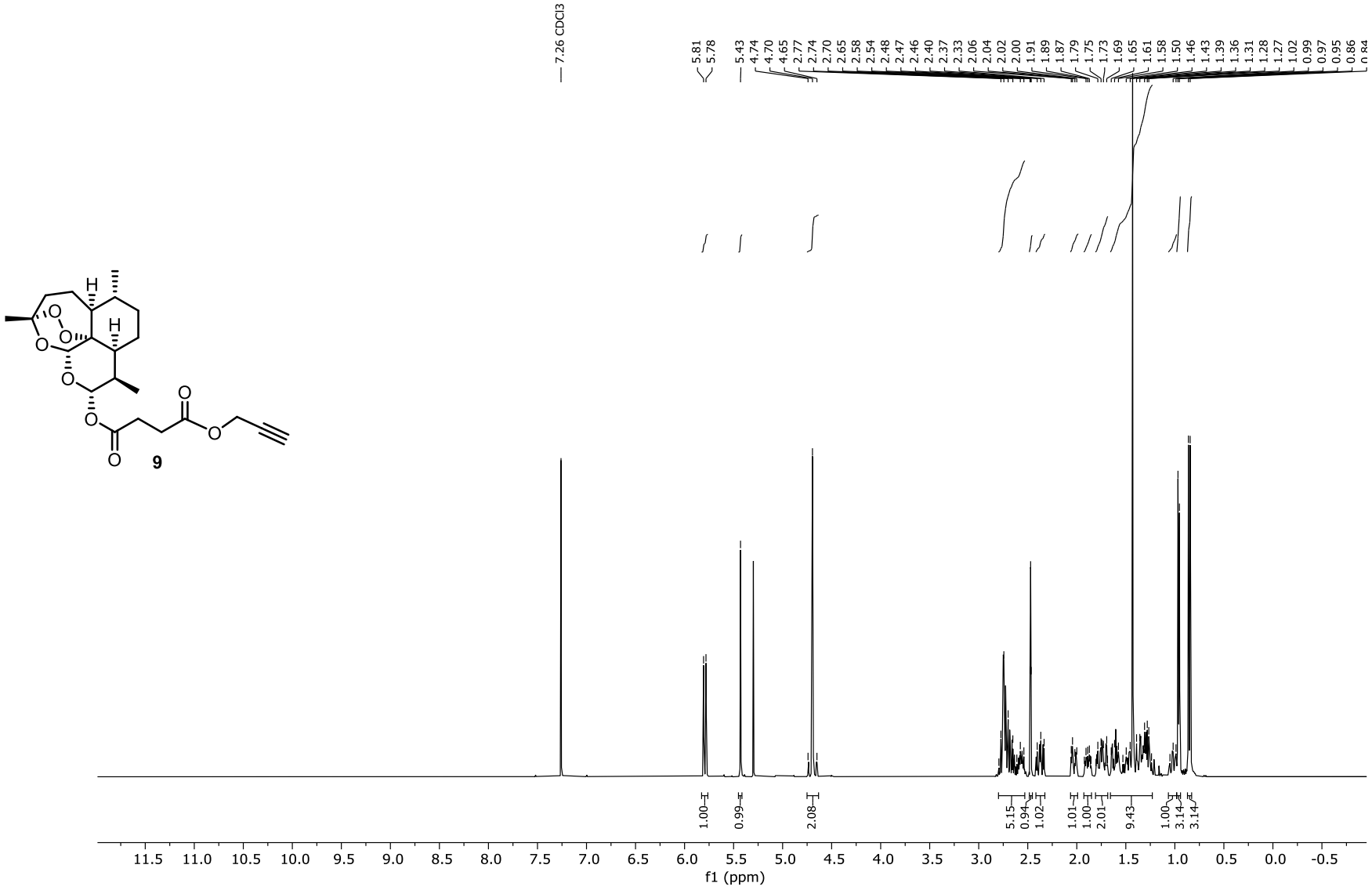

9

^{1}H NMR (400.35 MHz, DMSO-d6) of 2:

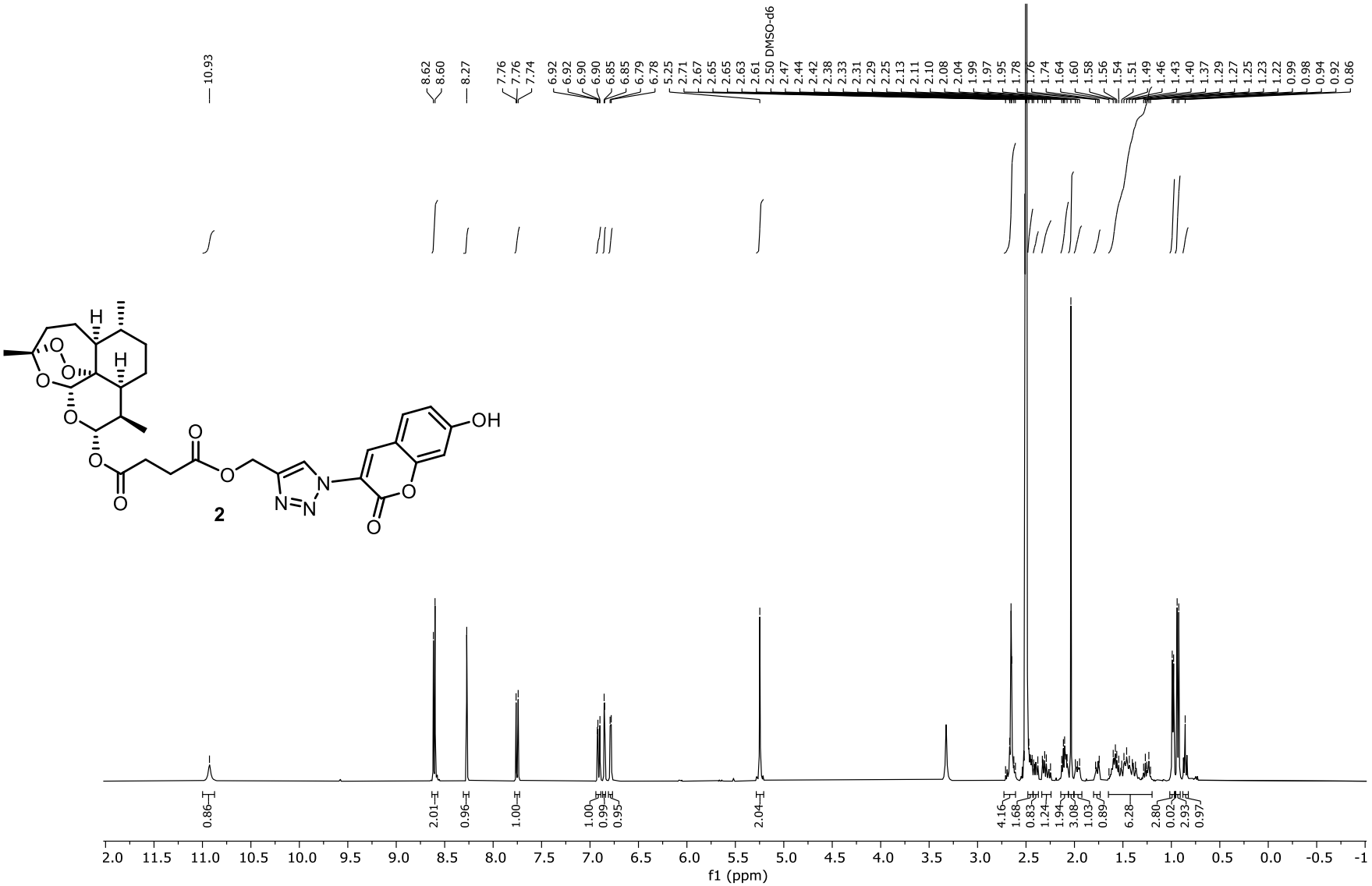

^{13}C NMR (100.68 MHz, $CDCl_3$) of 2:

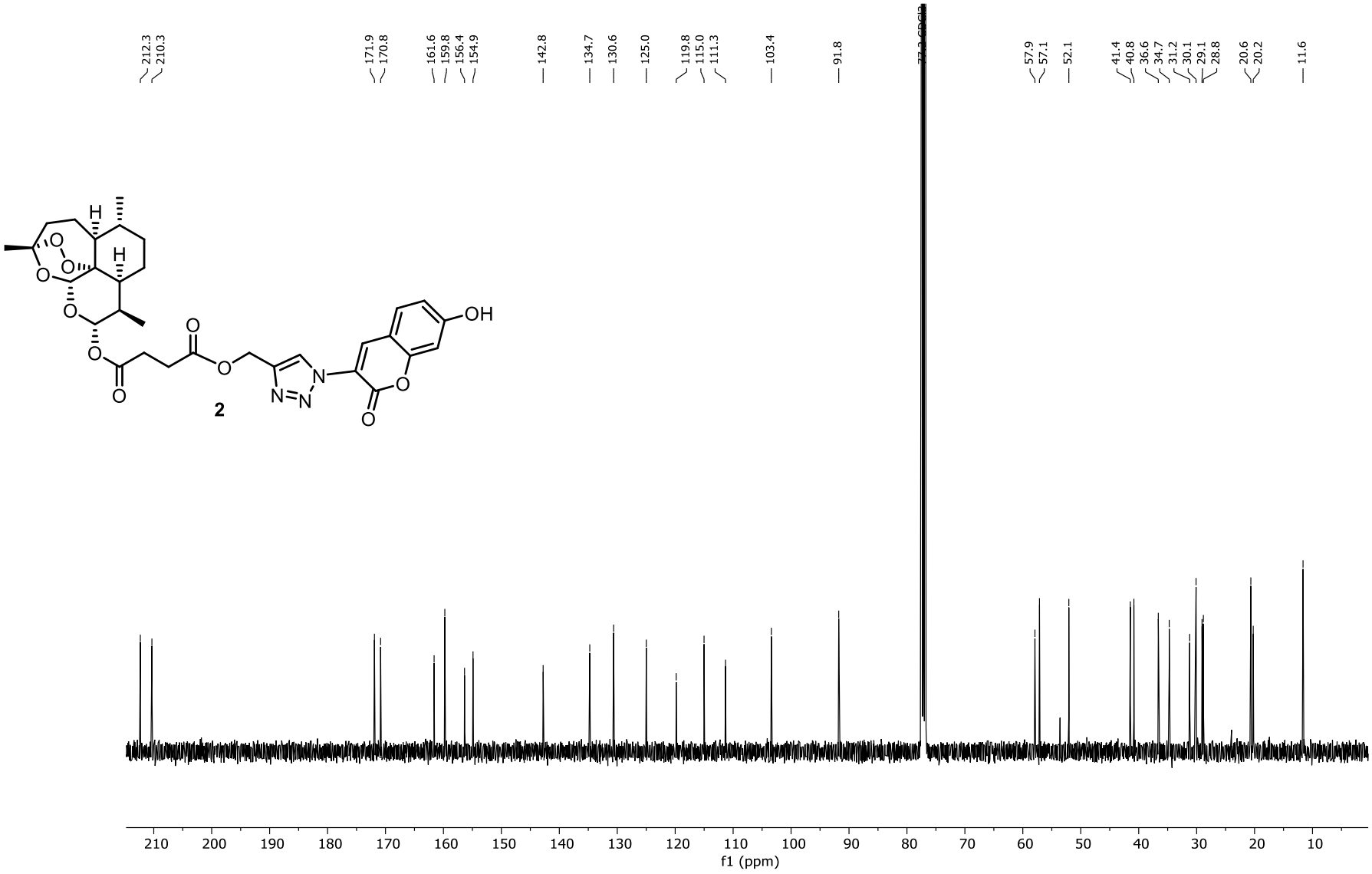

^{1}H NMR (400.35 MHz, $CDCl_3$) of 8:

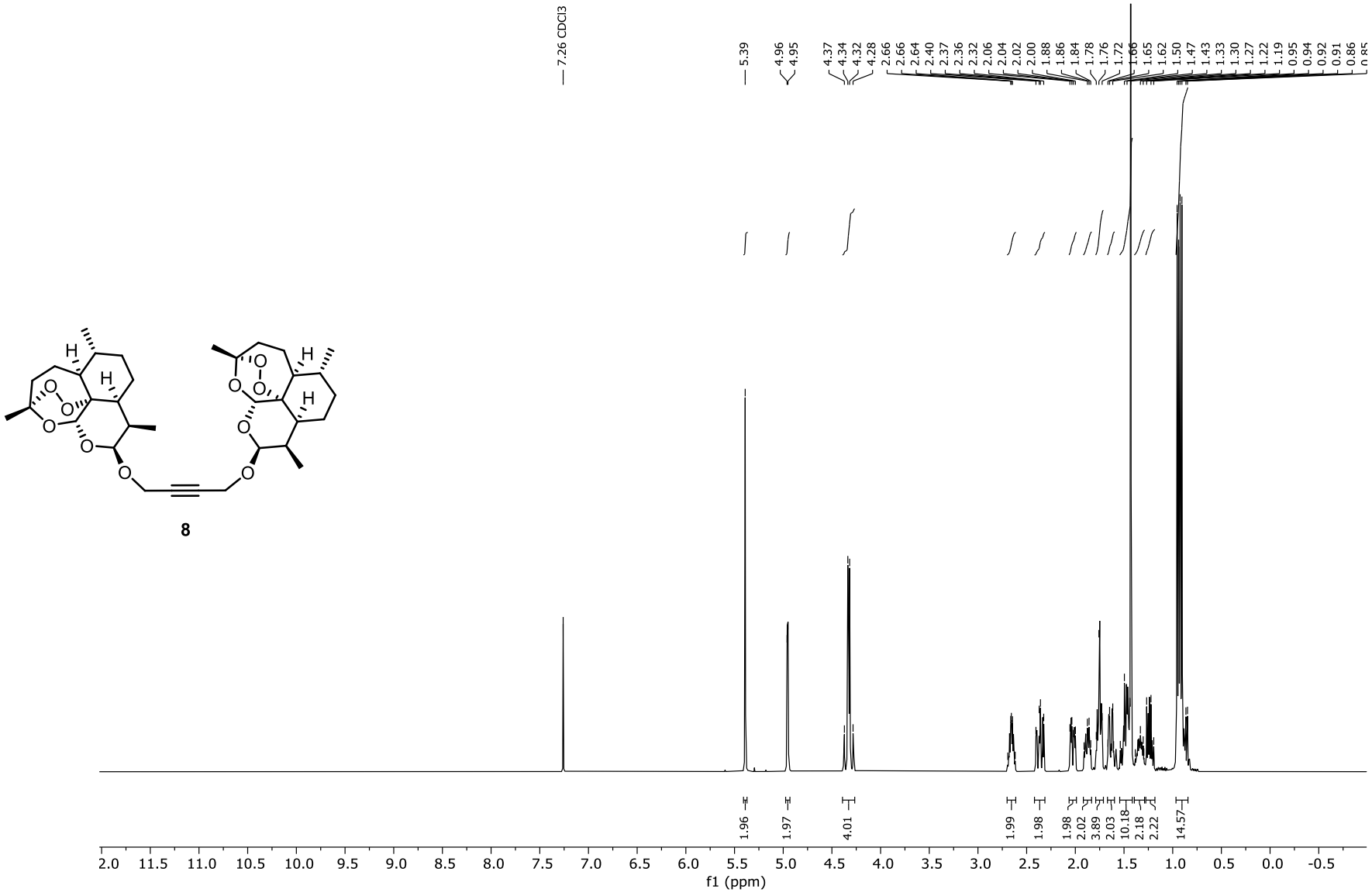

8

^{13}C NMR (100.68 MHz, $CDCl_3$) of 8:

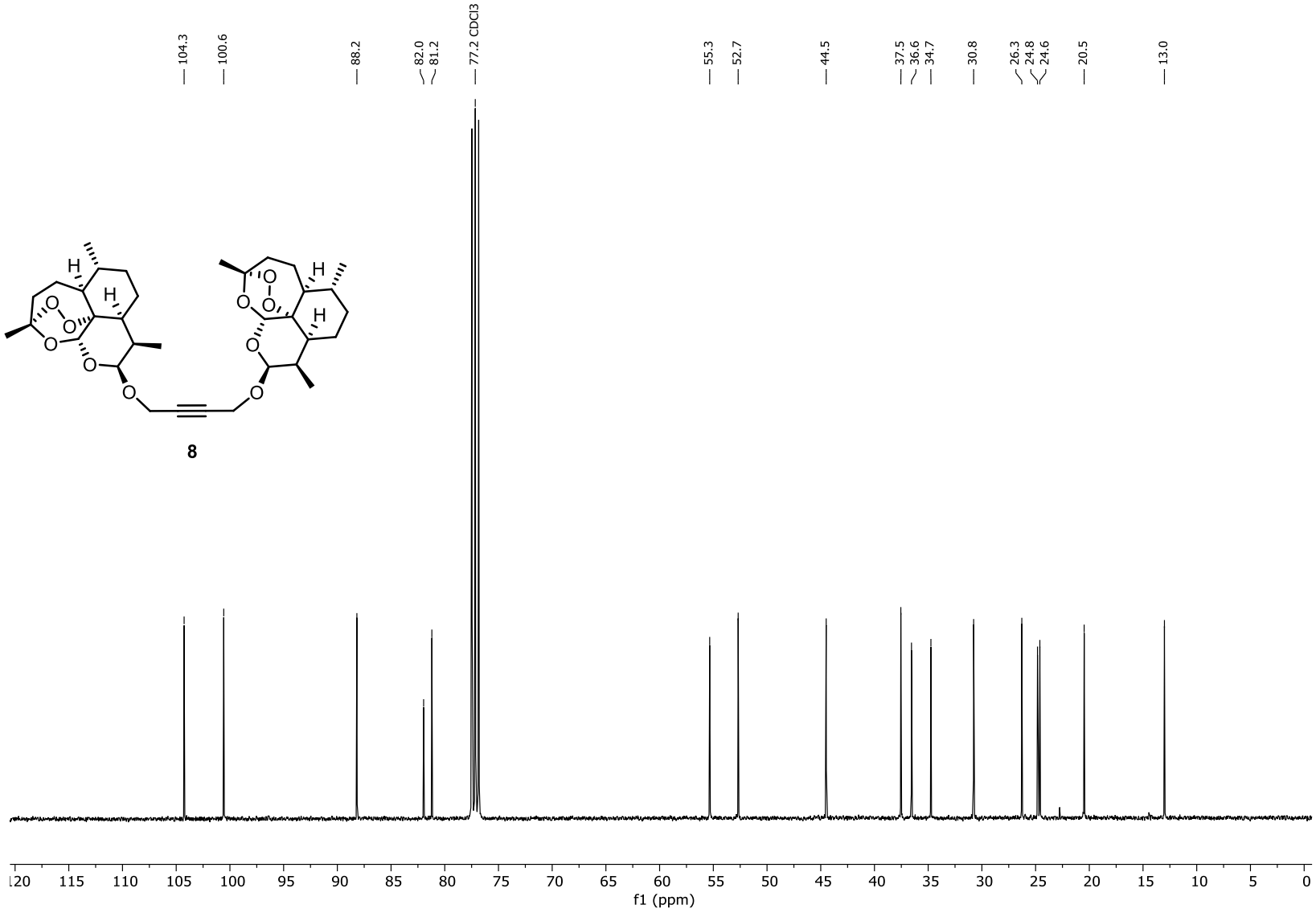

8

^{1}H NMR (400.35 MHz, DMSO-d6) of 3:

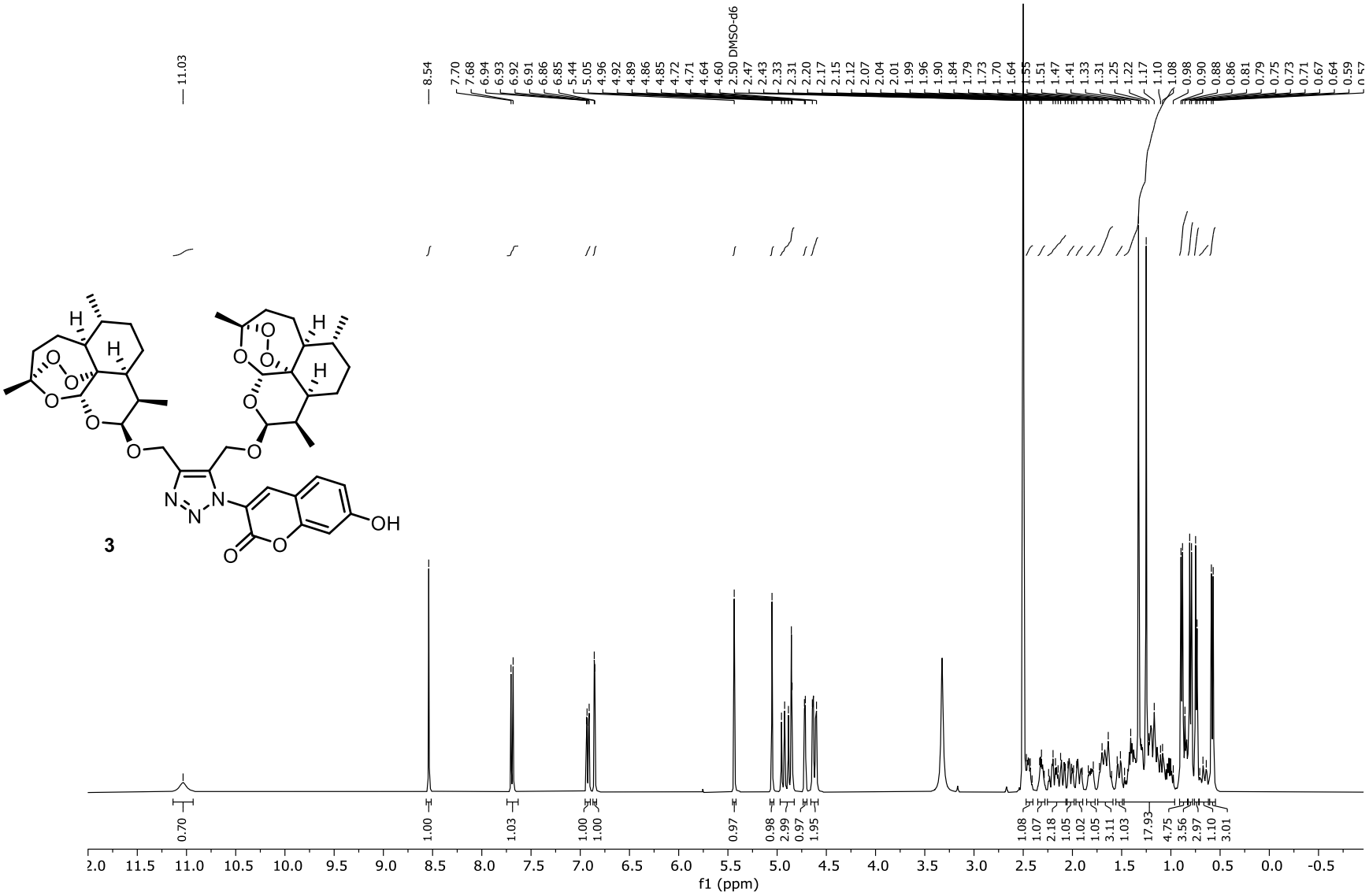

3

^{13}C NMR (100.68 MHz, $CDCl_3$) of 3:

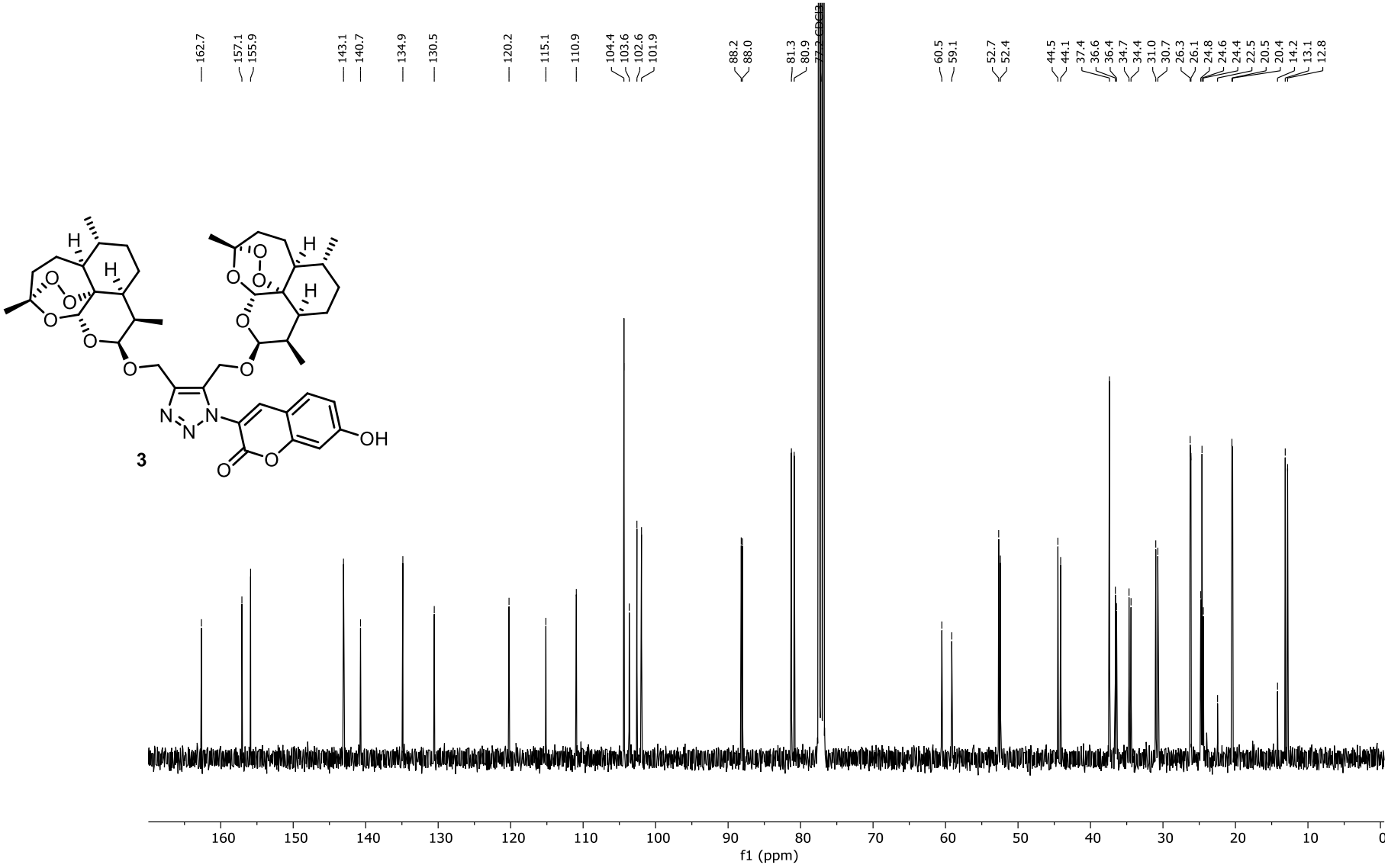

^{1}H NMR (400.35 MHz, DMSO-d6) of 4:

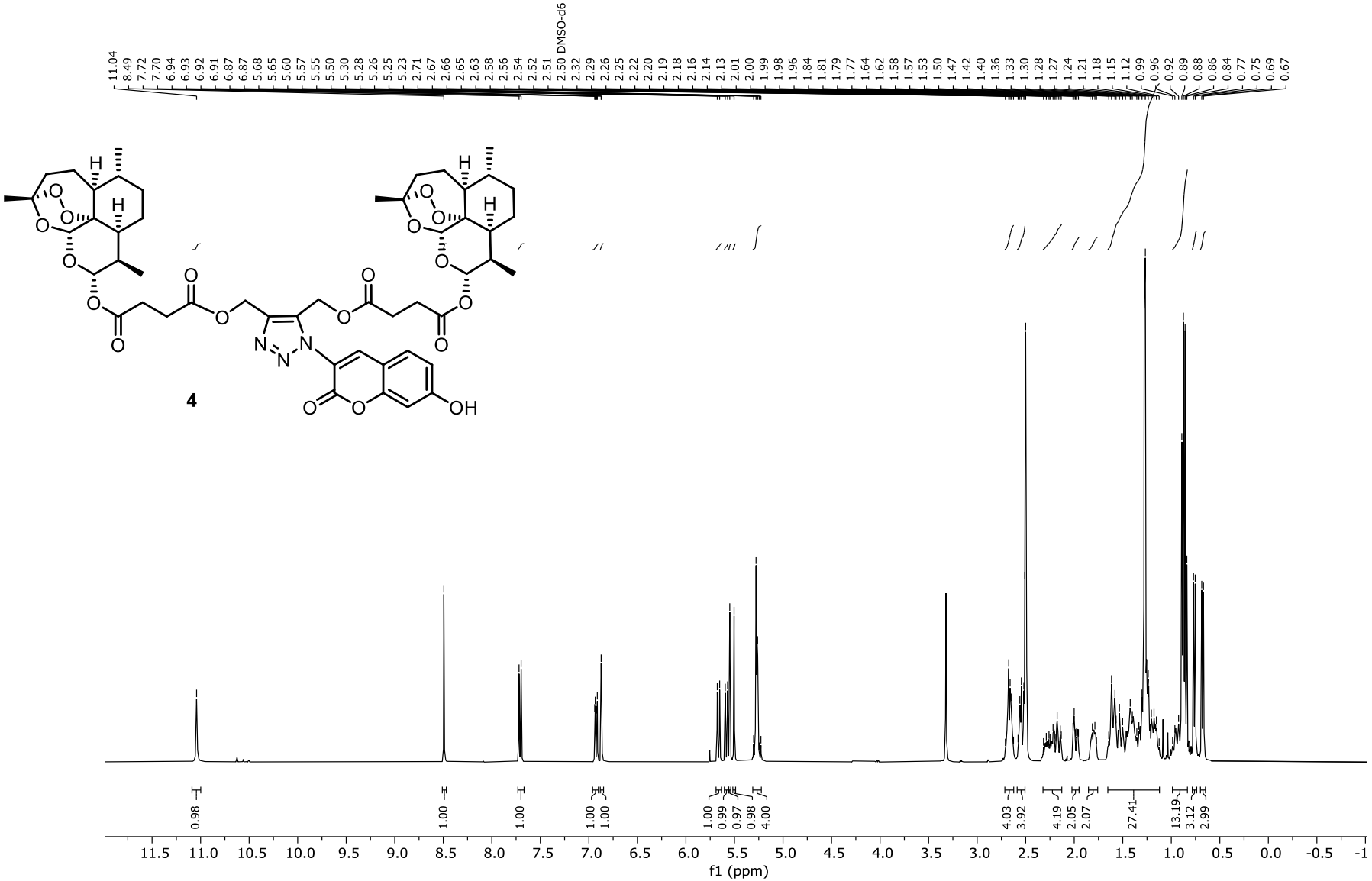

^{13}C NMR (100.68 MHz, DMSO-d6) of 4:

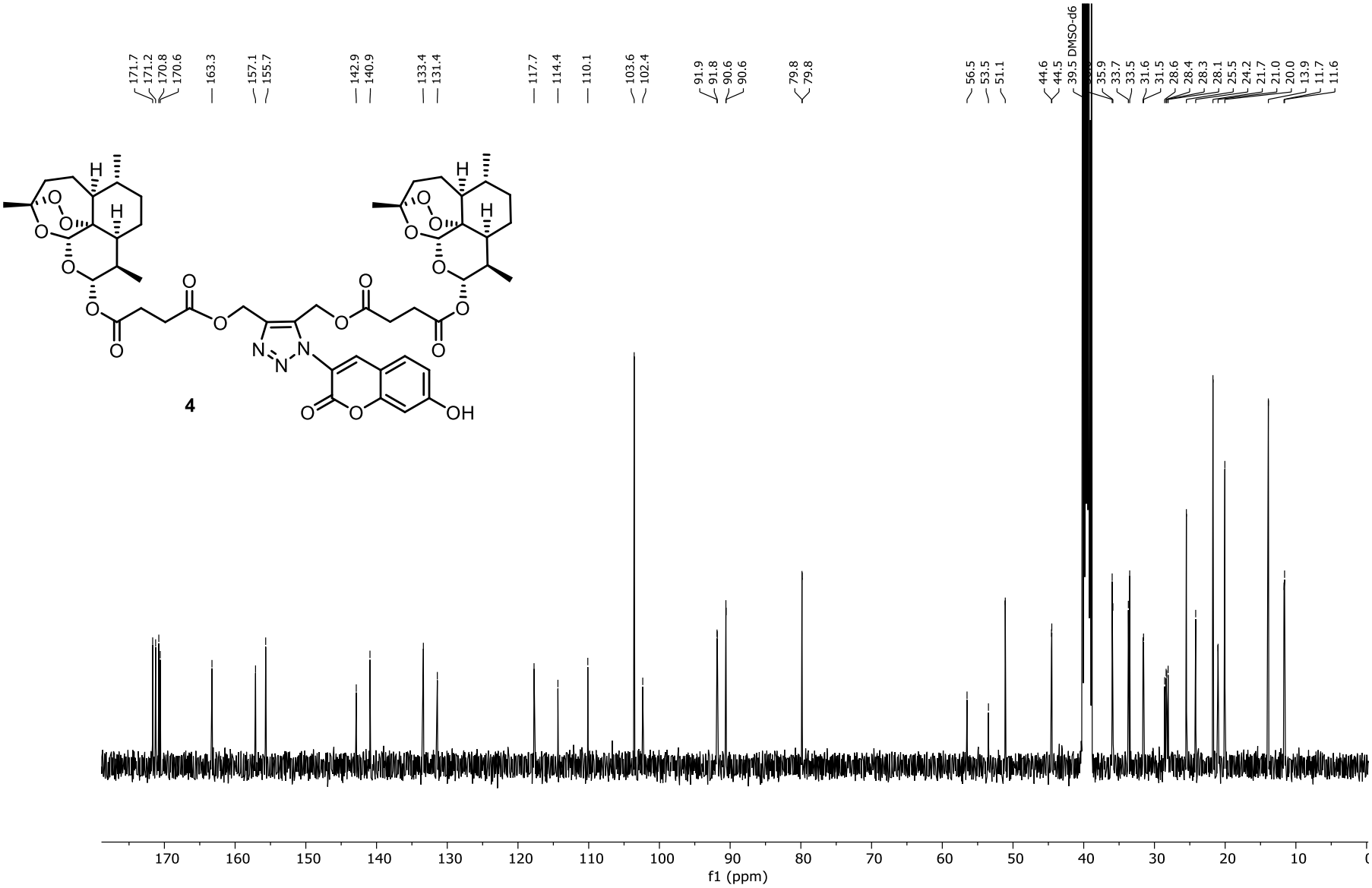

^{1}H NMR (400.35 MHz, DMSO-d6) of 5:

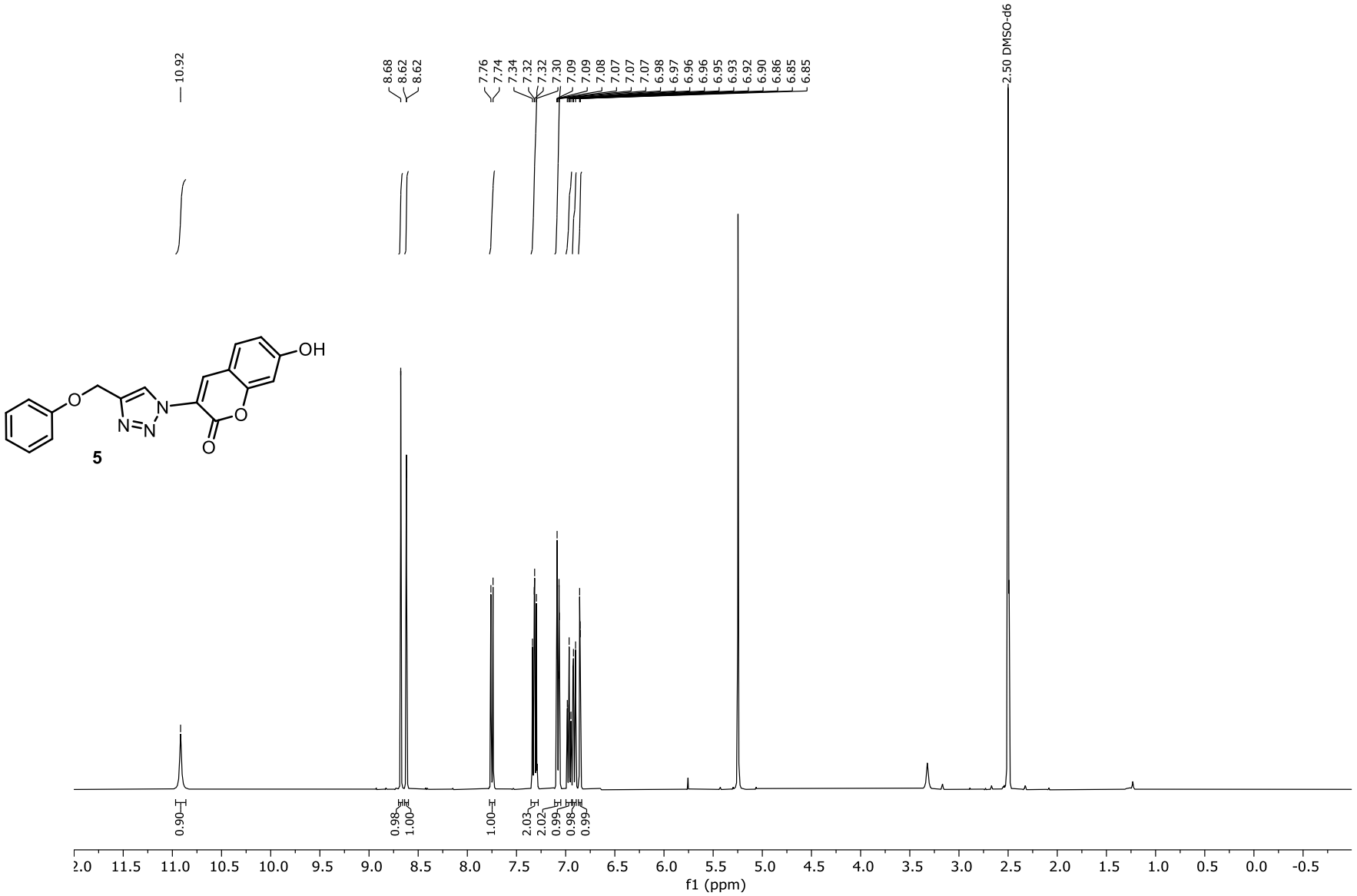

^{13}C NMR (100.68 MHz, DMSO-d6) of 5:

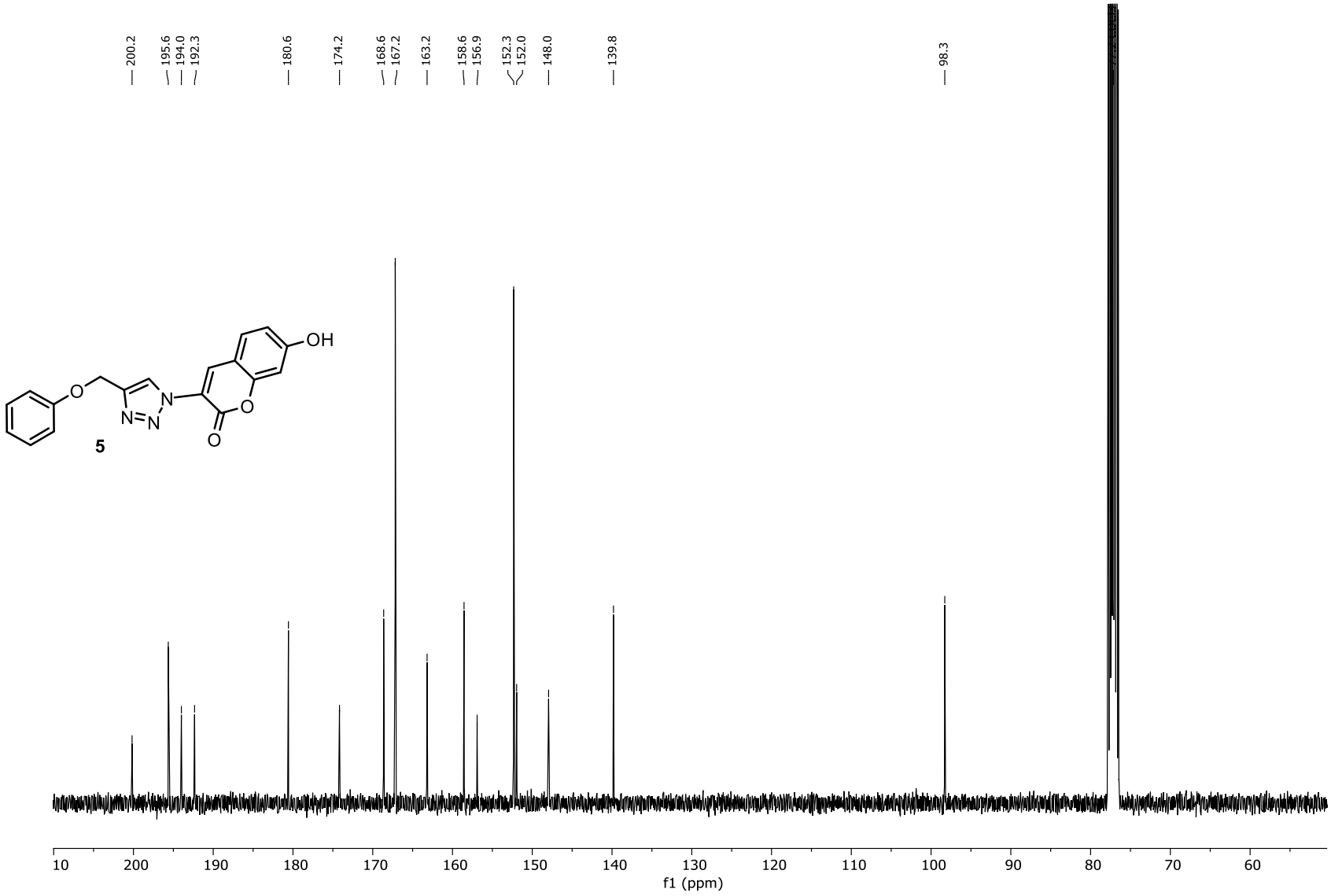

^{1}H NMR (400.35 MHz, DMSO-d6) of 6:

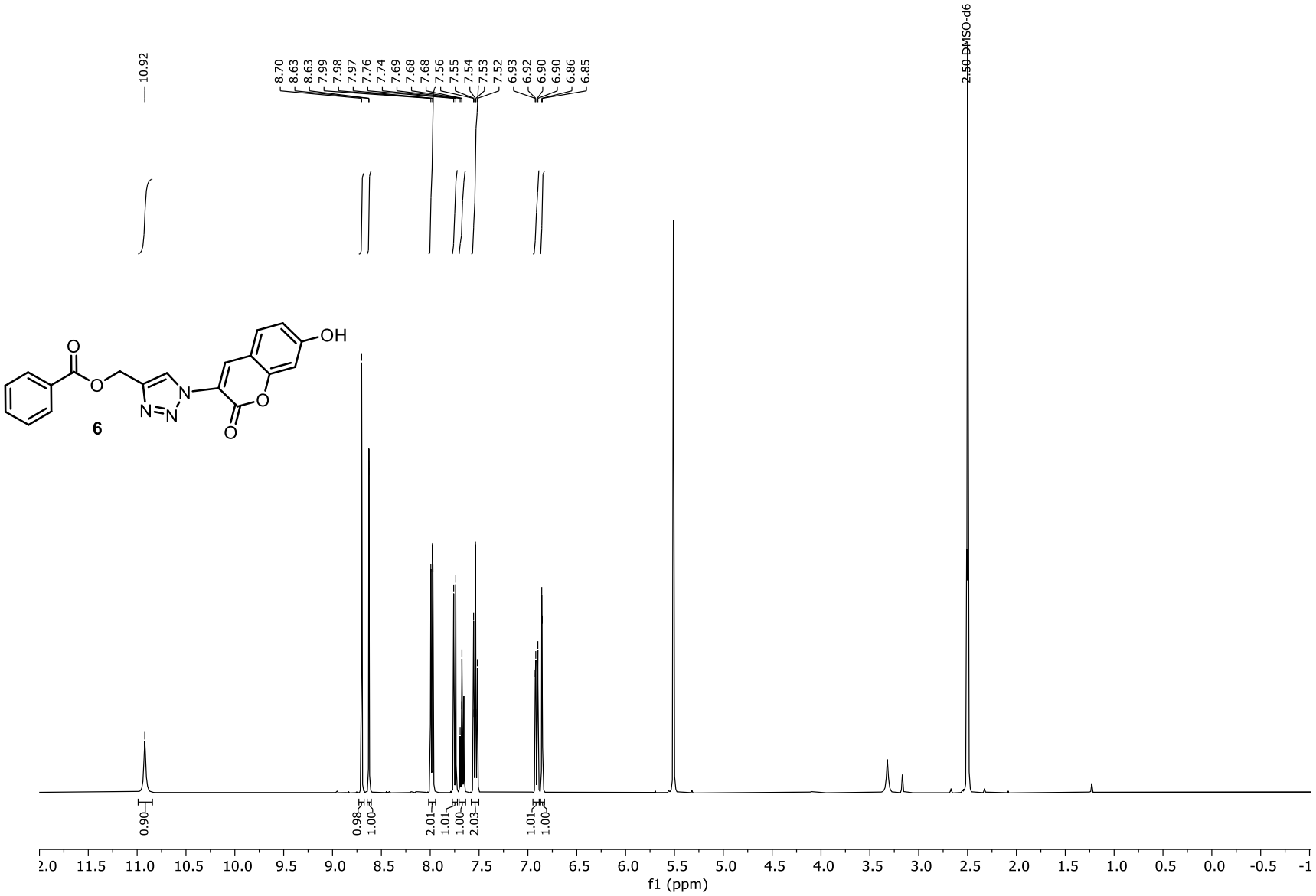

^{13}C NMR (100.68 MHz, DMSO-d6) of 6:

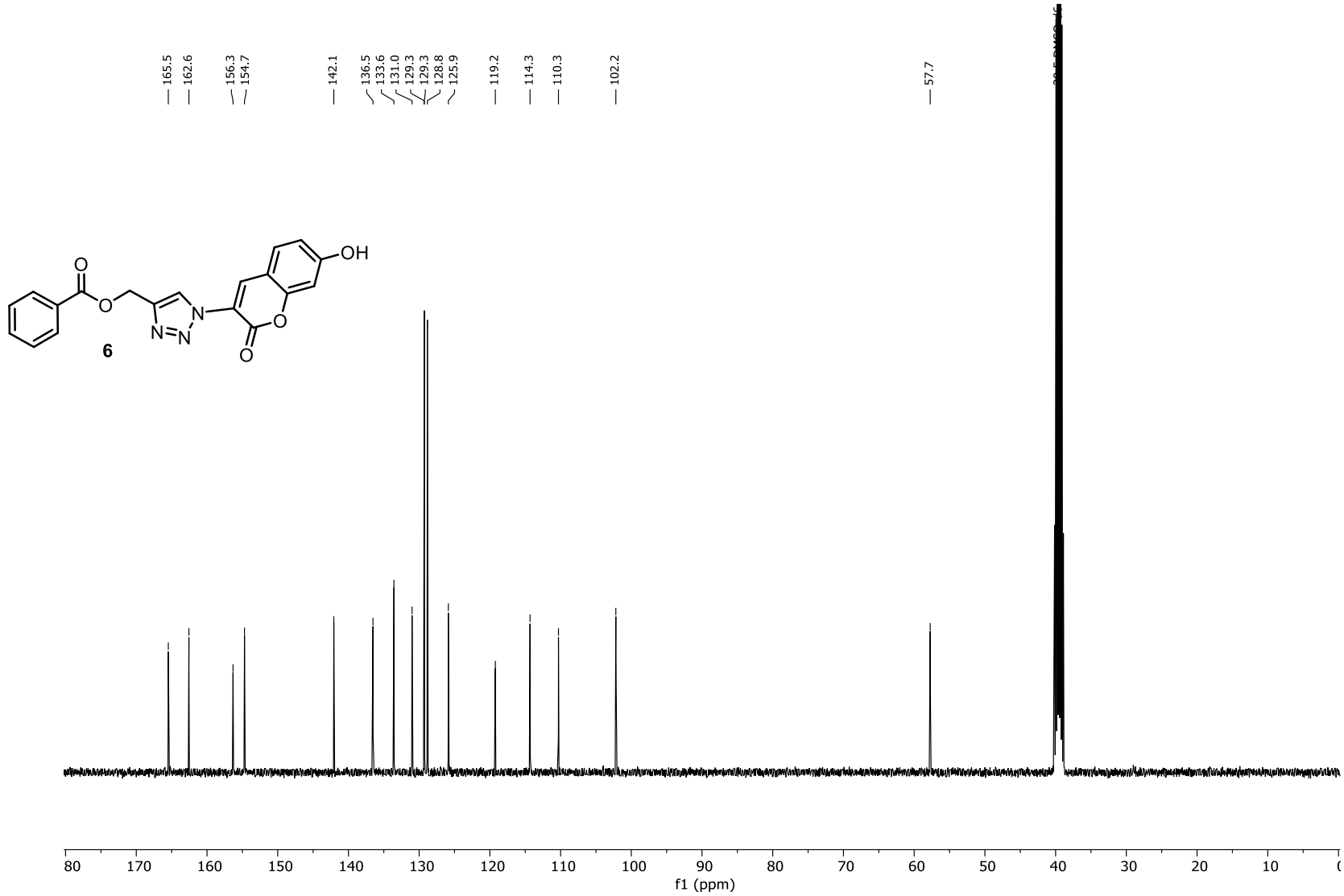

6. Stability testing of the hybrid compounds 1-6

To test the stability of the hybrid compounds 3-4 mg were dissolved in DMSO-d6 and a ^{1}H-NMR (400 MHz) was measured. The NMR tubes were than heated for 48 h at 60 C in an oil bath. None of the compounds showed a decomposition over 5%.

Stability test of hybrid **1**:

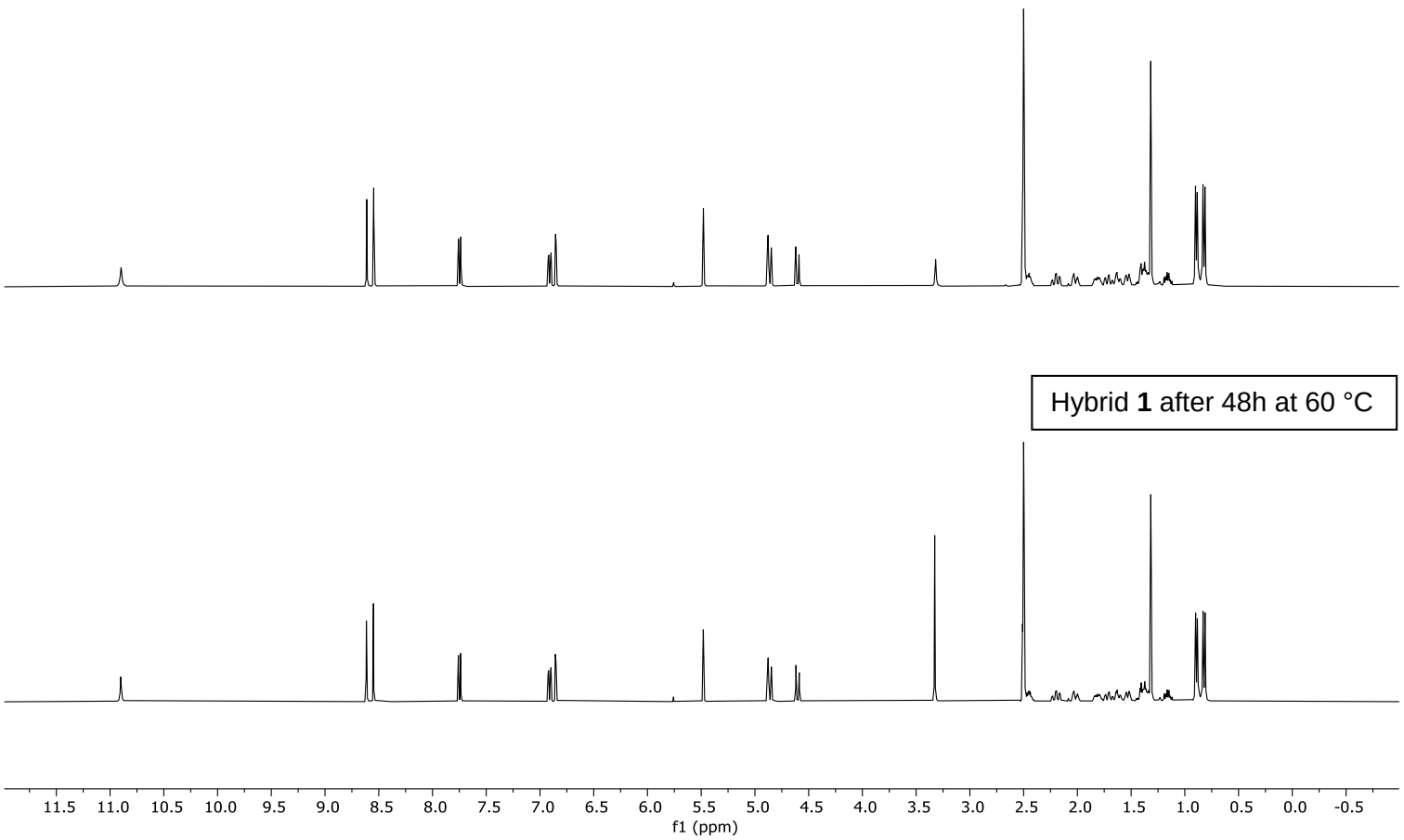

Stability test of hybrid **2**:

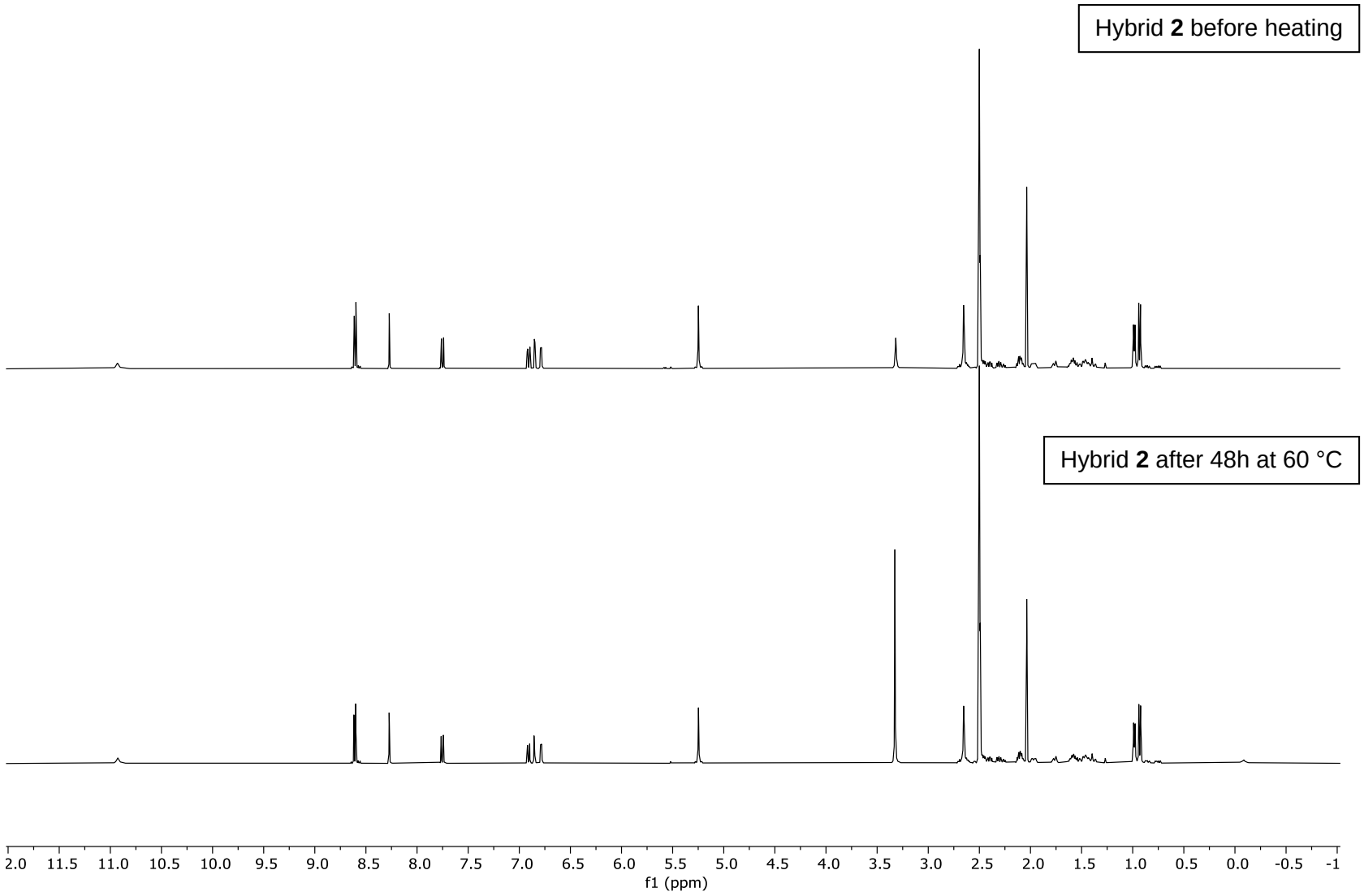

Stability test of hybrid **3**:

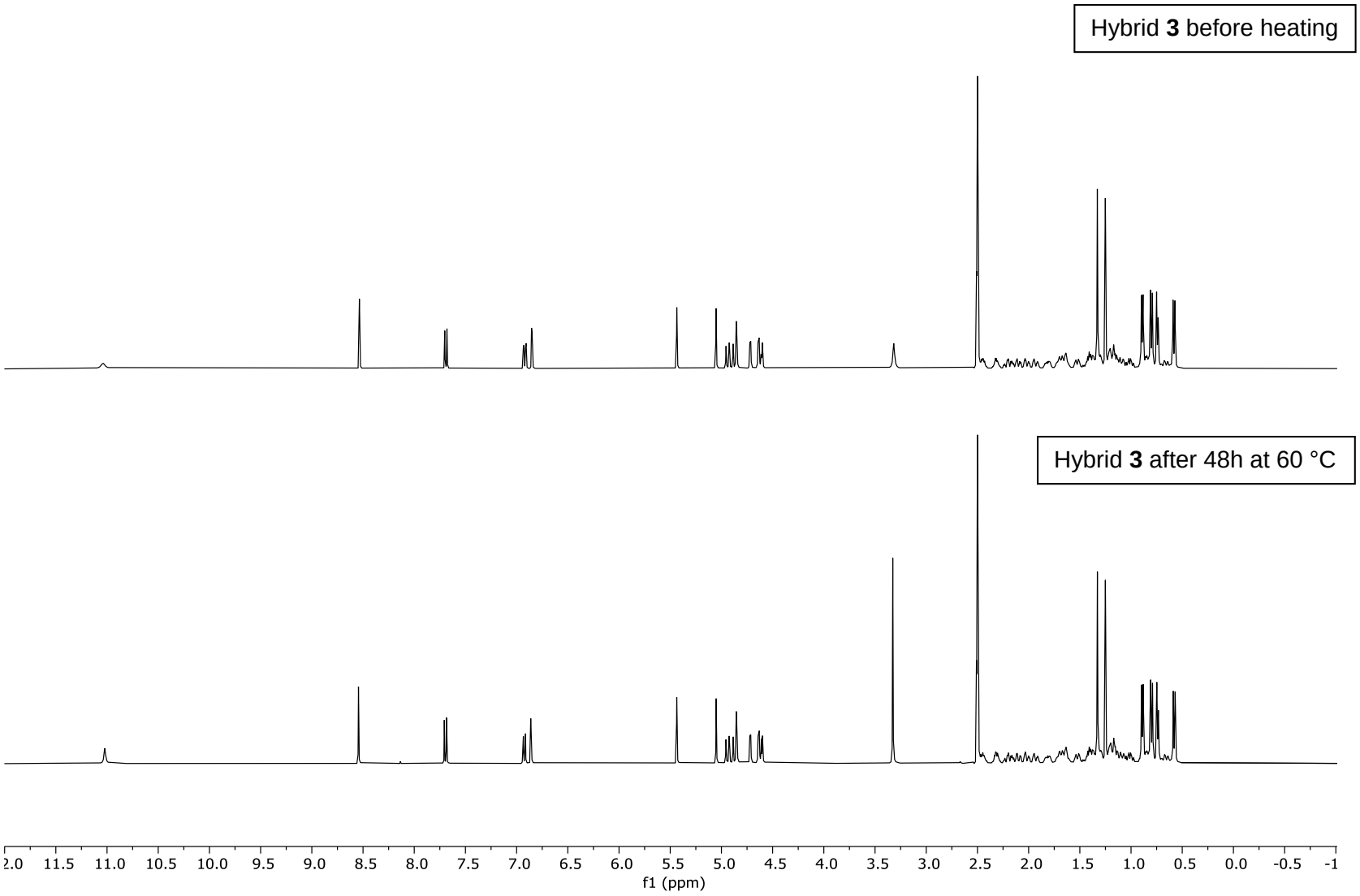

Stability test of hybrid **4**:

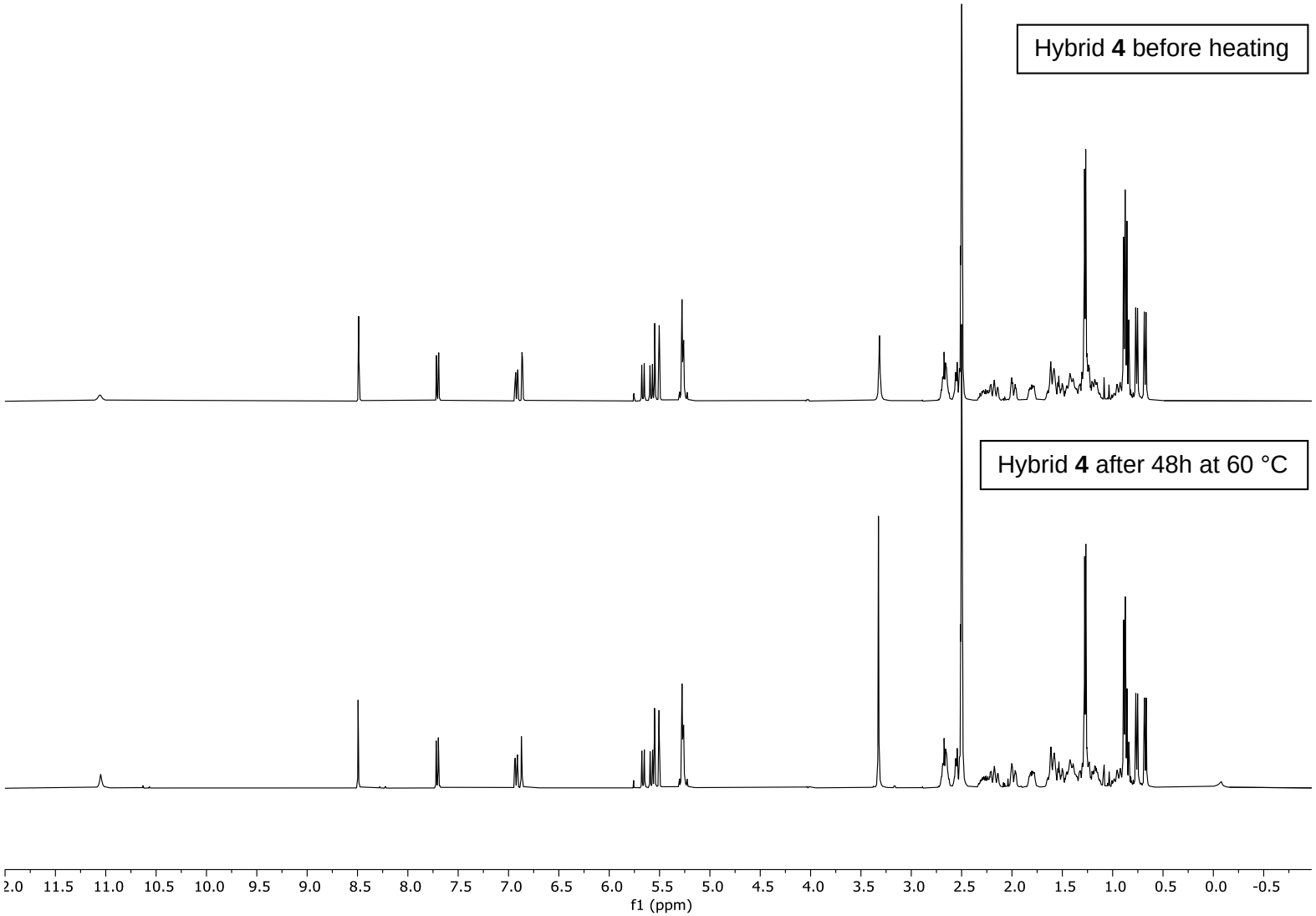

Stability test of compound **5**:

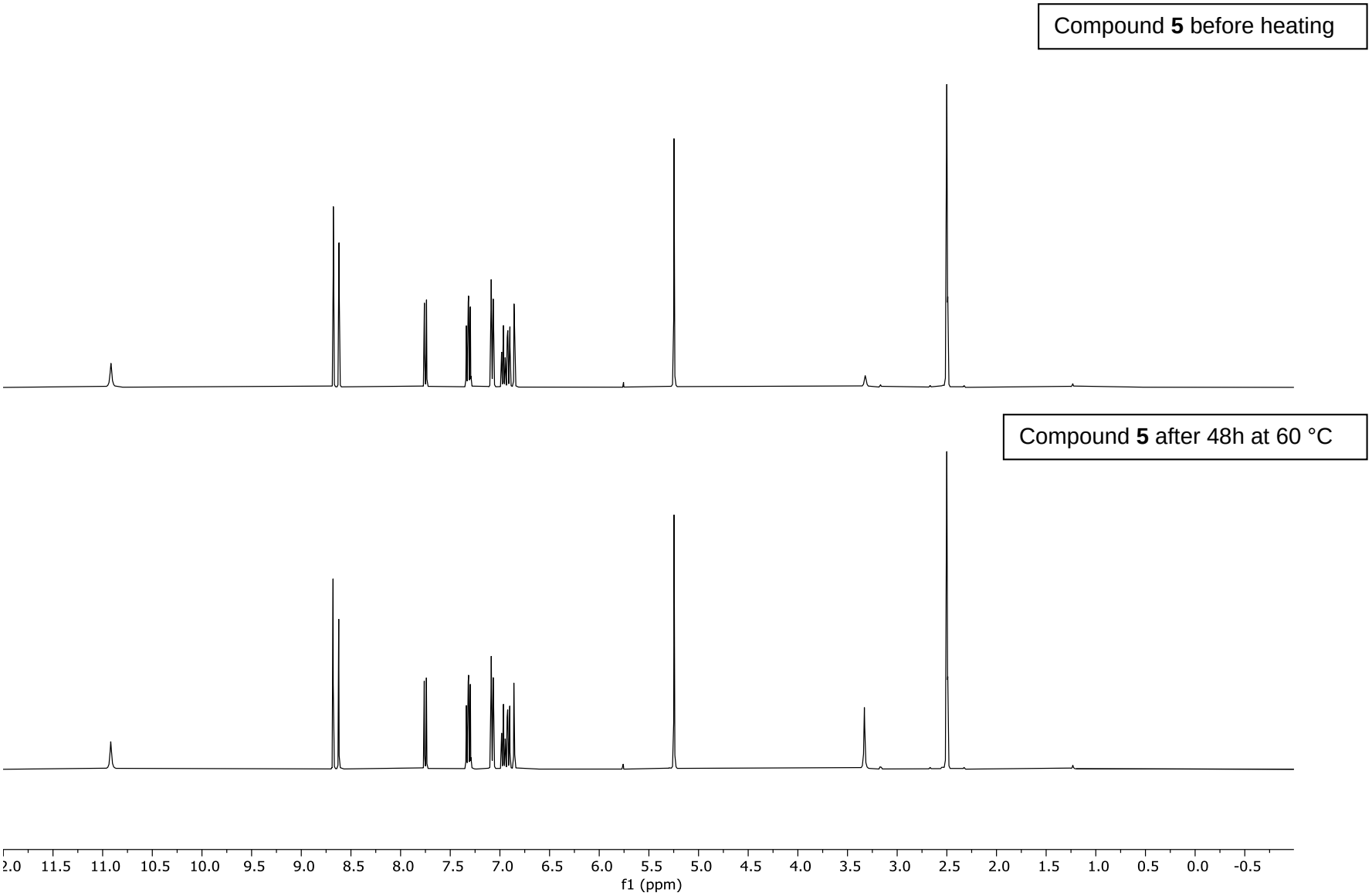

Stability test of compound **6**:

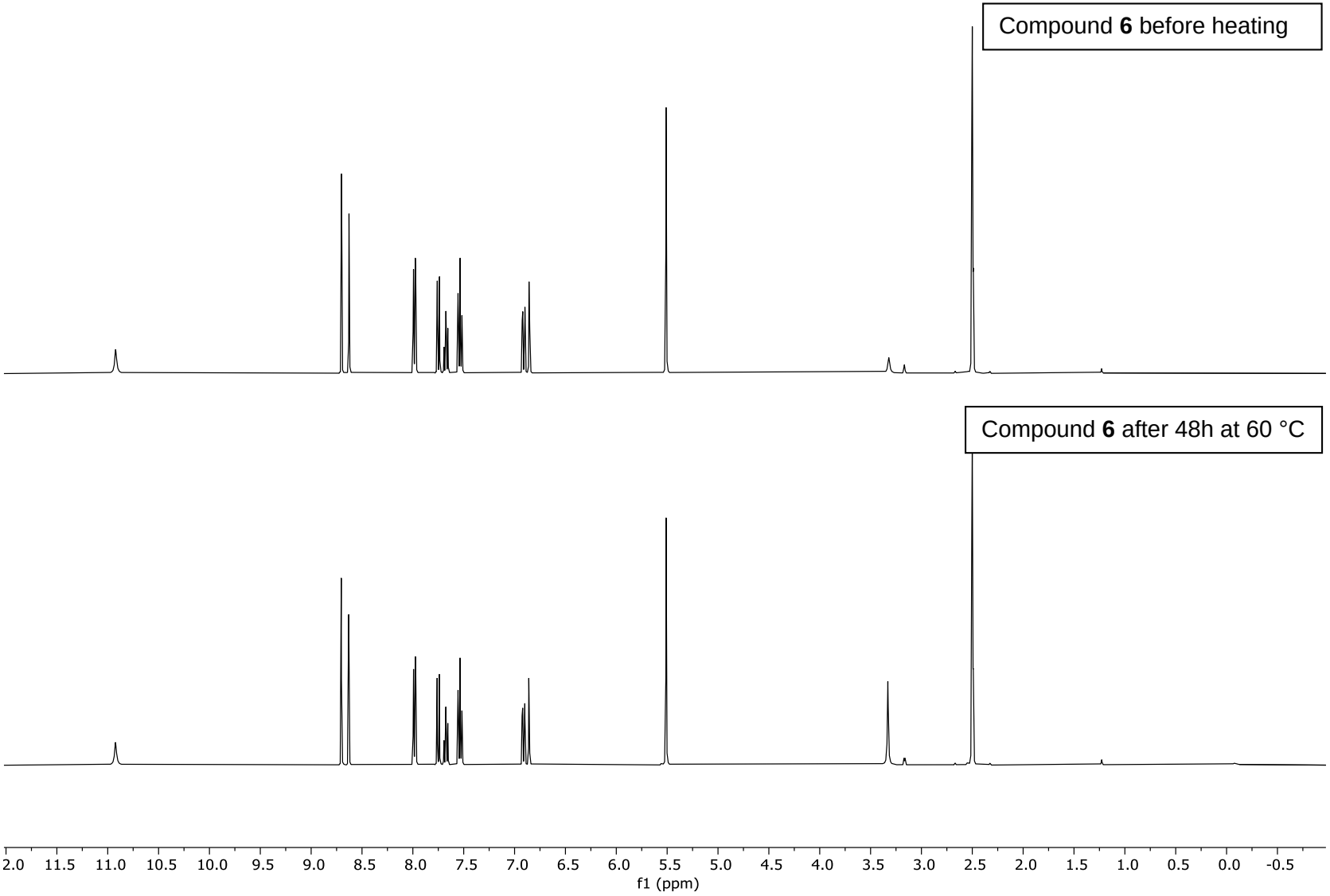

7. References

1 A. Çapcı, M. Lorion, H. Wang, N. Simon, M. Leidenberger, M. Borges Silva, D. Moreira, Y. Zhu, Y. Meng, J. Y. Chen, Y. Lee, O. Friedrich, B. Kappes, J. Wang, L. Ackermann and S. B. Tsogoeva, Artemisinin-(Iso)quinoline Hybrids by C-H Activation and Click Chemistry: Combating Multidrug-Resistant Malaria, *Angew. Chem. Int. Ed.*, 2019, **58**, 13066-13079.

2 P. P. Bora, N. Baruah, G. Bez and N. C. Barua, New Method for the Synthesis of Ether Derivatives of Artemisinin, *Synth. Commun.*, 2012, **42**, 1218-1225.

3 A. Çapcı, C. Reiter, E. J. Seo, L. Gruber, F. Hahn, M. Leidenberger, V. Klein, F. Hampel, O. Friedrich, M. Marschall, B. Kappes, T. Efferth and S. B. Tsogoeva, Access to new highly potent antileukemia, antiviral and antimalarial agents via hybridization of natural products (homo)egonol, thymoquinone and artemisinin, *Bioorg. Med. Chem.*, 2018, **26**, 3610-3618.

4 C. Lambros and J. P. Vanderberg, Synchronization of Plasmodium falciparum erythrocytic stages in culture, *J. Parasitol.*, 1979, **65**, 418-420.

5 M. Smilkstein, N. Sriwilaijaroen, J. X. Kelly, P. Wilairat and M. Riscoe, Simple and Inexpensive Fluorescence-Based Technique for High-Throughput Antimalarial Drug Screening, *Antimicrob. Agents Chemother.*, 2004, **48**, 1803-1806.

6 D. Beez, C. P. Sanchez, W. D. Stein and M. Lanzer, Genetic predisposition favors the acquisition of stable artemisinin resistance in malaria parasites, *Antimicrob. Agents Chemother.*, 2011, **55**, 50-55.

7 T. Yang, C. Xie Stanley, P. Cao, C. Giannangelo, J. McCaw, J. Creek Darren, A. Charman Susan, N. Klonis and L. Tilley, Comparison of the Exposure Time Dependence of the Activities of Synthetic Ozonide Antimalarials and Dihydroartemisinin against K13 Wild-Type and Mutant Plasmodium falciparum Strains, *Antimicrob. Agents Chemother.*, 2016, **60**, 4501-4510.

8 A. Sissoko, P. Vásquez-Ocmín, A. Maciuk, D. Barbieri, G. Neveu, L. Rondepierre, R. Grougnet, P. Leproux, M. Blaud, K. Hammad, S. Michel, C. Lavazec, J. Clain, S. Houzé and R. Duval, A Chemically Stable Fluorescent Mimic of Dihydroartemisinin, Artemether, and Arteether with Conserved Bioactivity and Specificity Shows High Pharmacological Relevance to the Antimalarial Drugs, *ACS Infect. Dis.*, 2020, **6**, 1532-1547.

9 A. T. R. Williams, S. A. Winfield and J. N. Miller, Relative fluorescence quantum yields using a computer-controlled luminescence spectrometer, *Analyst*, 1983, **108**, 1067-1071.

10 S. Hamai and F. Hirayama, Actinometric determination of absolute fluorescence quantum yields, *J. Phys. Chem.*, 1983, **87**, 83-89.